AD_____

AWARD NUMBER: W81XWH-08-1-0320

TITLE: Mechanisms of Abnormal Growth Regulation in Prostatic Adenocarcinoma Using Abi1/Hssh3bp1 Conditional Knockout Mouse Model

PRINCIPAL INVESTIGATOR: Leszek Kotula, M.D.
Xiaoling Xiong,.M.D.

CONTRACTING ORGANIZATION: New York Blood Center, Inc.
New York, NY 10021

REPORT DATE: June 2009

TYPE OF REPORT: Annual

PREPARED FOR: U.S. Army Medical Research and Materiel Command
Fort Detrick, Maryland 21702-5012

REPORT DOCUMENTATION PAGE

Form Approved
OMB No. 0704-0188

1. REPORT DATE	2. REPORT TYPE	3. DATES COVERED
1 June 2009	Annual	19 May 2008 – 18 May 2009

4. TITLE AND SUBTITLE

Mechanisms of Abnormal Growth Regulation in Prostatic Adenocarcinoma Using Abi1/Hssh3bp1 Conditional Knockout Mouse Model

5a. CONTRACT NUMBER

5b. GRANT NUMBER
W81XWH-08-1-0320

5c. PROGRAM ELEMENT NUMBER

6. AUTHOR(S)
Leszek Kotula, M.D., Xiaoling Xiong,.M.D

E-Mail: lkotula@nybloodcenter.org

5d. PROJECT NUMBER

5e. TASK NUMBER

5f. WORK UNIT NUMBER

7. PERFORMING ORGANIZATION NAME(S) AND ADDRESS(ES)

New York Blood Center, Inc.
New York, NY 10021

8. PERFORMING ORGANIZATION REPORT NUMBER

9. SPONSORING / MONITORING AGENCY NAME(S) AND ADDRESS(ES)
U.S. Army Medical Research and Materiel Command
Fort Detrick, Maryland 21702-5012

10. SPONSOR/MONITOR'S ACRONYM(S)

11. SPONSOR/MONITOR'S REPORT NUMBER(S)

12. DISTRIBUTION / AVAILABILITY STATEMENT
Approved for Public Release; Distribution Unlimited

13. SUPPLEMENTARY NOTES

14. ABSTRACT

Prostate cancer is the most common type of cancer found in American men. The American Cancer Society estimates that there will be about 190,000 new cases and 27,000 deaths of prostate cancer in the United States in 2009. Genetic alterations of tumor suppressor genes are one of the most common causes of prostate cancer tumorigenesis. Our group identified Abi1/Hssh3bp1 as candidate prostate tumor suppressor gene. To understand the role of Abi1/Hssh3bp1 in prostate tumorigenesis we developed the conditional Abi1/Hssh3bp1 KO mouse. In the first funding period we expanded our mouse colony and set up specific breeding schemes for proposed prostate tumorigenesis mouse models i.e. for prostate-specific disruption of Abi1/Hssh3bp1 or simultaneous disruption of Abi1/Hssh3bp1 and PTEN genes. Cre recombinase-mediated disruption of the gene was confirmed in dissected prostates of animals with Abi1/Hssh3bp1 (fl/fl)PbCre(Tg/-) genotype. In addition we isolated Abi1/Hssh3bp1 (fl/fl) MEF cells and cloned cells lacking Abi1/Hssh3bp1 to be used for in vitro characterization of Abi1/Hssh3bp1-dependent cell growth regulation pathways. Toward that goal we also screened genome-wide SH2 domain library with phosphotyrosine peptides derived from Abi1/Hssh3bp1 and identified several candidate Abi1/Hssh3bp1-binding SH2 domain-containing proteins. These protein-Abi1/Hssh3bp1 interactions will be further characterized using cells and animal tissue lacking Abi1/Hssh3bp1.

15. SUBJECT TERMS
mouse model, tumor biology, cell growth, tumor suppression, tumorigenesis, molecular genetics

16. SECURITY CLASSIFICATION OF:			17. LIMITATION OF ABSTRACT	18. NUMBER OF PAGES	19a. NAME OF RESPONSIBLE PERSON
a. REPORT	b. ABSTRACT	c. THIS PAGE			USAMRMC
U	U	U	UU	70	19b. TELEPHONE NUMBER *(include area code)*

Table of Contents

Introduction

Prostate cancer is now the most common type of cancer found in American men. One out of six American men develop prostate cancer. The American Cancer Society estimates that there will be about 190,000 new cases of prostate cancer in the United States in 2009. About 27,000 men will die of this disease this year. However, the health prospective of men diagnosed with prostate cancer is improving: the death rate for prostate cancer is going down primarily because the disease is being detected at earlier stages before the cancer has metastasized. Recent significant advancements in understanding prostate biology, genetic interactions of tumor suppressor genes, and the dynamics of cancer progression have been made using mouse models for prostate cancer. These models include Nkx3.1, p53, p27, and also Pten, a gene, which is mutated in most prostatic adenocarcinoma cases. Although it is generally agreed that genetically engineered mouse models do not resemble all features of human prostate pathology, they do offer great promise for anti-cancer drug development. Mouse models also offer significant advantage over xenograft models, as they much more faithfully recapitulate developmental stages of cancer progression.

In this research we propose to characterize the novel Abi1/Hssh3bp1 conditional knock-out mouse model in the prostate, a model developed by our laboratory. Identification of primary prostate tumor mutations in Abi1/Hssh3bp1 strongly supports the hypothesis that the gene acts as tumor suppressor. The original work of our laboratory also identified a novel mechanism of growth regulation that involves allosteric regulation of c-Abl tyrosine kinase. Our functional studies of prostate cancer mutations suggest that loss of Abi1/Hssh3bp1 function leads to dysregulated c-Abl kinase activity, enhanced cell proliferation and spreading, and subsequently to prostate tumorigenesis. Dysregulated c-Abl kinase activity has been implicated in various forms of leukemia, thus leading us to hypothesize that prostate tumorigenesis may involve similar mechanisms. Addressing this hypothesis using the Abi/Hssh3bp1 conditional knock-out mouse model will likely have high impact on the prostate cancer research field including development of novel potential drug therapies. Our model will also allow testing of genetic interactions of multiple tumor suppressor genes, a situation frequently observed in human pathology.

In the first funding period we expanded our mouse colony for this study and set up specific breeding schemes for proposed prostate tumorigenesis mouse models. These include models for heterozygous and homozygous prostate-specific disruption of Abi1/Hssh3bp1 gene alone as well as for simultaneous disruption of both PTEN and Abi1/Hssh3bp1 genes. The prostate-specific probasin promoter-driven Cre recombinase-mediated disruption of the gene was confirmed in dissected prostates of Abi1/Hssh3bp1 (fl/fl)PbCre (+/-) animals. In addition we isolated Abi1/Hssh3bp1 (fl/fl) MEF cells and cloned cells lacking Abi1/Hssh3bp1 to be used for in vitro characterization of Abi1/Hssh3bp1-dependent cell growth regulation pathways. Toward that goal we also screened genome-wide SH2 domain library with Abl tyrosine kinase dependent phosphotyrosine peptides derived from Abi1/Hssh3bp1 and identified several candidate Abi1/Hssh3bp1-binding SH2 domain-containing proteins. These protein-Abi1/Hssh3bp1 interactions will be further characterized using cells and animal tissue lacking Abi1/Hssh3bp1 to determine its role in cell growth and cell signaling.

Body

"Mechanisms of Abnormal Growth Regulation in Prostatic Adenocarcinoma Using Abi1/Hssh3bp1 Conditional Knockout Mouse Model"

Introduction. This project is performed in the Laboratory of Cell Signaling at the Lindsley F. Kimball Research Institute (LFKRI) of the New York Blood Center (NYBC), New York. Considering time needed to breed enough animals for histopathological evaluation of proposed mouse models we focused our research efforts on expanding the mouse colony (Aim 1), as well as we initiated Aims 2 and 3 of the project.

Below are listed Specific Aims of the grant as originally stated under **Statement of Work**

Task 1. To determine histological and phenotypical changes in the mouse prostate following prostate-specific disruption of Abi1/Hssh3bp1 (Months 1-36). We plan to evaluate 390 experimental (experimental model mice including controls) and 26 wild type mice under *Task 1*.

a. To obtain conditional knockout of Abi1/Hssh3bp1 in the prostate by breeding Abi1/Hssh3bp1 $^{+/loxP}$ or Abi1/Hssh3bp1 $^{loxP/loxP}$ mice with Pb Cre mice.

b. To determine expression pattern of Abi1/Hssh3bp1 and mouse prostate histology in heterozygous and homozygous Abi1/Hssh3bp1 KO mice (Months 18-36).

c. To determine expression pattern and mouse prostate histology of Abi1/Hssh3bp1/PTEN double knockout mice (Months 24-36).

Task 2. To determine tumorigenicity of LnCAP-Abi1/Hssh3bp1 cell lines stably transfected with prostate tumor mutations using xenograft model system. (Months 1-12). We plan to use 96 mice in for the tumorigenicity studies.

a. To obtain stable LnCAP cell lines transfected with the wild type and prostate tumor mutants of Abi1/Hssh3bp1/Hssh3bp1 (Months 1-4). To characterize LnCAP-Abi1/Hssh3bp1 cell lines using cell growth, apoptosis, and cell spreading assays (Months 6-8).

b. To determine tumorigenicity of LnCAP-Abi1/Hssh3bp1 cell lines using xenograft model system (Months 8-12).

Task 3. To determine candidate molecular mechanisms of Abi1/Hsshb3p1-depedent growth regulation *in vivo* by examination of c-Abl kinase activity, and identification of proteins binding to pY213 of Abi1/Hssh3bp1, using LNCaP cells and MEF cells from Abi1/Hsshb3p1 KO as model systems (Months 24-36).

a. To determine c-Abl kinase activity in LnCAP-Abi1/Hssh3bp1 stable cell lines and in mouse embryonic fibroblasts isolated from conditional Abi1/Hssh3bp1 KO mouse. (Months 24-32).

b. To determine candidate Abi1/Hssh3bp1 signaling pathways by identification of proteins binding to pY213. (Months 24-36).

Progress toward Aim 1 (Task 1)

Recapitulation of Aim 1 goals. The goal of Aim1 is to evaluate by histopathology the prostate-specific disruption of Abi1/Hssh3bp1 gene alone or together with PTEN gene. To achieve this we needed to expand the mouse colony to produce enough animals for downstream breeding. At the time of funding the project by DOD the Abi1/Hssh3bp1 floxed/floxed (or Abi1/Hssh3bp1 (fl/fl)) mouse was already available in our laboratory. This strain does not have a neomycin gene in the recombinant Abi1/Hssh3bp1 gene cassette. The neomycin gene removal was accomplished by breeding of the original Abi1/Hssh3bp1 transgene mouse with the frt deletor strain (129S4/SvJaeSor-Gt(ROSA)26Sortm1(FLP1)Dym/J, The Jackson Laboratories). We also obtained PTEN (fl/fl) strain 129S4-Ptentm1Hwu/J (The Jackson Laboratories) to be used for Model 3 breeding. We are continuing to expand our mouse colony.

The breeding effort in the first year included the following:

1. Production of Abi1/Hssh3bp1 (fl/fl) females for downstream breeding to produce the proposed mouse models.
2. Production of Abi1/Hssh3bp1 (fl/+)PbCre(Tg/-) males to be used for breeding of Model 1 and Model 2.
3. Expansion of PTEN (fl/fl) strain and initiation of breeding schemes for Model 3.

Here is recapitulation of our mouse models:

1.Model 1- Prostate-specific knockout of one Abi1/Hssh3bp1 allele
1.1 Control Mice for Model 1: Abi1/Hssh3bp1$^{loxP/+}$;PB-Cre$^{-/-}$ male sibs from above cross.
2. Model 2 - Prostate-specific knockout of two alleles of Abi1/Hssh3bp1
2.1 Control Mice for Model 2: Abi1/Hssh3bp1$^{loxP/loxP}$ males.
3. Model 3 - Prostate-specific knockout of one Abi1/Hssh3bp1 allele in Pten $^{-/-}$ mouse (LNCaP-like)
3.1 Control mice for Model 3: Abi1/Hssh3bp1$^{loxP/loxP}$/Pten$^{-/-}$ male mice.

Progress. We have now over 30 male mice for each group under observation for Model 1 and Model 2 and for their appropriate corresponding controls. We are continuing to breed the animals for these models to obtain enough animals for evaluation at planned time points of evaluation (65 mice for each group). Evaluation of Model 1 and 2 will take most of the second and part of the third funding period. Model 3 requires much more initial breeding than the first two models. The critical intermediate mouse strain here is the "doubly" floxed Abi1/Hssh3bp1(fl/fl)/PTEN(fl/fl) strain; the breeding of this strain is currently underway. Once enough females of Abi1/Hssh3bp1(fl/fl)/PTEN(fl/fl) strain are obtained we will initiate breeding males for Model 3 i.e. prostate deletion of Abi1/Hssh3bp1 and PTEN.

Evaluation of Abi1/Hssh3bp1 knockout mice. Breeding of mice to obtain specific knockouts is being done at the animal colony at NYBC, which meets federal guidelines and is under the care of a veterinarian and trained personnel. Molecular and genetic evaluation of mice will be done in our laboratory using standard techniques. The histopathological evaluation of mice will be done in collaboration with the Histology Laboratory of Memorial Sloan Kettering Cancer Center (MSKCC), located near our laboratory at NYBC's East 67th Street, Manhattan, facility. Male mice will be evaluated for the presence of primary tumors in the prostate and presence of metastatic growth in other tissues.

Progress toward Aim 2 (Task 2).

Recapitulation of Aim 2 goals. The goal of this Aim is to evaluate the role of identified primary prostate mutations (that we presented as preliminary data for this grant) in regulation of cell growth using xenograft tumor model. Xenograft tumor models provide rapid assay to evaluate proliferation/apoptosis potential of cell lines in situ expressing various forms of a protein in question. In principle, the xenograft model is a complementation assay: we will test whether stable expression of the wild type Abi1/Hss3bp1 in contrast to the mutated protein suppresses tumorigenicity of LNCaP cells. In addition, we will evaluate cell growth and cell spreading characteristics of these cell lines to determine their tumorigenic potential and the candidate growth pathway in vitro. This information will be very useful in evaluating the role of primary tumor mutations *in vivo* and such studies provide parallel data regarding the role of potential molecular mechanism identified *in vitro* culture system in the dynamics and tumorigenic potential *in vivo*. Here we have a situation nearly ideal for such studies. Our laboratory demonstrated in the past that LNCaP cells contain heterozygous Abi1/Hssh3bp1 mutation (Macoska et al., 2001), hence levels of Abi1/Hssh3bp1 protein are very low. The LNCaP cell line has been one of the most extensively used cell lines for xenograft as well for in vitro studies.

Progress: We have introduced the following mutations into the plasmid vectors expressing wild type isoform 2 Abi1/Hssh3bp1: truncating mutations at residue 330; 351 and amino acid replacements P412S, P418S, and S297N. We have previously established cell lines expressing wild type of Abi1/Hssh3bp1, and Y213F and ^{182}AESEA^{187} mutants of Abi1/Hssh3bp1. Using these established cell lines we performed cell growth assays.

Caveats and problems: Using available cell lines we performed initial experiments of cell growth using two types of assays: growth assay using cell plated on plastic dishes or using soft agar assay. Data from plastic dishes and soft agar assay suggest different differences in growth regulation. Clones expressing Abi1/Hssh3bp1 wt demonstrated better growth than the mutant Y213F expressing cells in soft agar, while on plastic dishes it they grew very similar and slower than mock control. Interestingly, Abi1/Hssh3bp1 wt clone showed enhanced response (in comparison to Y213F mutant) to the growth factor PDGF on plastic. In addition we noted substantial differences in cell spreading abilities between the clones: Abi1 expressing wt showed decreased spreading ability vs. Y213F mutant on dishes. Based on our paper Xiong et al 2008 we hypothesize that Abi1/Hssh3bp1 plays a role in Abl kinase regulation and the Y213 plays a critical role in Abl kinase activity. We are performing more experiments to understand the growth regulation mechanism involving Y213 in conjunction with c-Abl kinase regulation.

Progress toward Aim 3 (Task 3)

Recapitulation of Aim 3 goals. The goal of this Aim is to determine candidate molecular mechanisms of Abi1/Hssh3bp1-depedent growth regulation by examination of c-Abl kinase activity and by identification of proteins binding to pY213 of Abi1/Hssh3bp1 (pY213 is the major tyrosine phosphorylation site by c-Abl). We plan to achieve these goals by achieving the following goals:

1. Aim 3a - is to examine cellular growth pathways affected by disruption of Abi1/Hss3hbp1 gene using MEF cells lacking the gene. We hypothesized here that lack of Abi1/Hssh3bp1 dysregulates c-Abl kinase activity.

2. Aim 3b - is to determine candidate Abi1/Hssh3bp1 signaling pathways by identification of proteins binding to pY213.

Progress. We have made rapid progress toward achieving Aim 3 goals. First of all we successfully isolated MEF cells from Abi1/Hssh3bp1 floxed mouse and removed the Abi1/Hssh3bp1 gene in vitro. Initial assays indicate enhanced proliferation of cells lacking the gene using mitochondrial dehydrogenase (Dubielecka et al, manuscript under preparation, attached). The attached manuscript draft entitled "Phenotypic Characterization of Cells Lacking Abi1/Hssh3bp1 Gene" describes all the steps from production of the transgenic Abi1/Hssh3bp1 strain to initial characterization of cellular phenotype of MEF cells. Abi1/Hssh3bp1 is part of the so-called Wave complex, a multiprotein complex that regulates actin polymerization, hence the manuscript describes findings regarding the actin cytoskeleton phenotype that we observe in MEF cells. The original production of the strain was supported by the start up funds to our laboratory as well as by a grant from the F.M. Kirby Foundation. The current DOD grant is focusing on characterization of cell growth phenotype related to removal of Abi1/Hss3hbp1 gene and will be our focus in subsequent funding periods i.e. Year 2 and Year 3 of the grant.

We also made progress toward Aim 3b. The goal of this Aim is to identify potential downstream targets of Abi1/Hssh3bp1 phosphotyrosine 213 (pY213). Screening of genome-wide SH2 domain library identified candidate targets of Abi1/Hssh3bp1-pY213 that include regulatory subunit of PI-3 kinase p85. We have performed genome-wide screening studies to identify candidate-binding targets for Abi1/Hssh3bp1 pY213. pY213 had consensus for SH2 domain binding and its binds with moderate affinity to Abl SH2 domain as demonstrated in our paper (Xiong et al., 2008). Hence library containing SH2 domains was used in the screening. These experiments were done in collaboration with Dr. Bruce Mayer and Dr. Machida (University of Connecticut Health Science Center, Farmington, CT) using the overlay method developed by Dr. Mayer laboratory (Machida et al., 2007). Candidate proteins containing SH2 domain were identified in the screening and following the screening candidate binding partners were evaluated for binding affinity to pY213 containing peptide (pY213v2) and pY421 containing peptide (pY421) (Table 1, and attached report). Both screening result and affinity constant indicate that Abl-SH2 domain is indeed a good ligand for pY212 among many other SH2 domains but there are multiple SH2 domains with higher affinity than Abl SH2 domain including Arg, CblB, and Vav2. Most notably pY213 bound to p85 regulatory subunit of PI3 kinase. Based on this result we have formed a hypothesis PI3 kinase is downstream of Abi1/Hssh3bp1 pY213 phosphorylated by Abl kinase. Further studies are being developed to test this hypothesis. The document describing the screening and all results is attached.

Table. 1 Affinities of candidate Abi1/Hssh3bp1 binding proteins identified in pY screening

	Kd (nM)	
SH2	pY213v2	pY421
Abl	1259	UD
mAbl	725.3	UD
Arg	25.08	844.5
Lck	1207	36.42
Src	UD	612.5
FynA	UD	108.2
Frk	UD	329.7
CblB	19.52	UD
CrkL	106.8	UD
Nap4	UD	UD
p85α(NC)	134.8	240.6
Vav2	23.19	255
Sck/ShcB	148.7	UD
Fer	UD	UD
Gap(NC)	441.5	UD
PLCγ1(NC)	UD	UD

UD, undefined

Key Research Accomplishments

◆ **We established Abi1/Hssh3bp1 floxed strain in our laboratory.**

◆ **We isolated mouse embryonic fibroblasts or MEF cells from Abi1/Hssh3bp1 conditional KO mouse. Cells lacking Abi1/Hssh3bp1 display enhanced proliferation.**

◆ **We identified p85 regulatory subunit of PI-3 kinase as candidate Abi1/Hssh3bp1 binding protein in the phosphotyrosine-SH2 domain screen using pY213 and pY421 of Abi1/Hssh3bp1 probes. Based on this finding we formed a hypothesis that PI-3 kinase is a downstream target of phospho-Abi1. PI-3 kinase is the critical pathway dysregulated in prostate cancer.**

Reportable Outcomes

1. Manuscripts:

1-1. Dubielecka, P.M., Schloen, K.S., Xiong, X., Vedvyas, Y., Rottner, K., Stradal, T., and L. Kotula. Phenotypic Characterization of Cells Lacking Abi1/Hssh3bp1 Gene. *Manuscript under preparation – see attached draft (Appendix).*

2. Invited talks:

2-1. Invited talk: Kotula, L., "Regulation of Abl kinase activity by Abi1/Hssh3bp1: why we need Abi1/Hssh3bp1 KO mouse" Department of Physiology and Biophysics, Stony Brook University, New York June 10, 2009.

2-2. Invited talk at the international meeting "Membrane Skeleton - Research Advances and Future Research Directions ", June 15-18, 2008, Zakopane, Poland: Kotula, L.. "Allosteric inhibition of the nonmyristoylated c-Abl tyrosine kinase by phosphopeptides derived from ABI1/HSSH3BP1"

3. New Funding Applied for /Obtained:

3-1. The grant entitled "Development of Mouse Model of Prostate Cancer" was funded by F.M. Kirby Foundation. This is a renewal application - grant was renewed this year.

3-2. NIH/NIGMS **9R01 GM087739-05** grant application entitled "Regulation of Macropinocytosis by Hssh3bp1" was submitted. This is a renewal application. Kotula, L (PI).

3-3. NIH/NCI Mouse Models**: RFA-CA-08018:** ***Integration of Mouse Models into Human Cancer Research (U01)*** grant application: "Cancer biology of Abi1/Hssh3bp1 knockout mouse model" Kotula, L (PI) was submitted.

4. Development of mouse cell lines and plasmids. Abi1/Hssh3bp1 conditional KO mouse strain, MEF cell lines obtained from the Abi1/Hssh3bp1 KO mouse as well as any developed plasmid expressing Abi1/Hssh3bp1 will be available to scientific community upon publication of the results of this work.

Conclusions

Two major conclusion of the presented progress of work are:

1. Abi/Hssh3bp1 is an inhibitor of cell growth – based on our findings from cell lacking Abi1/Hssh3bp1 gene.

2. Abi1/Hssh3bp1 may be involved in PI-3 kinase pathway – based on the phosphotyrosine screening and identification of p85 regulatory subunit of PI-3 kinase as candidate binding protein.

Significance and relevance of our findings for prostate cancer research. Here, we propose to characterize the novel Abi1/Hssh3bp1 conditional knock-out mouse model, which was developed by our laboratory. To the best of our knowledge, we are the only group to have made this model. Specifically, we propose to conditionally disrupt the gene in the mouse prostate and evaluate whether this results in histopathological changes characteristic of prostate tumors in mice. The proposed studies stem from our initial identification of potential involvement of Abi1/Hsshb3p1 in prostate cancer tumorigenesis. With previous funding from the DOD CDMRP program, we identified *Abi1/Hssh3bp1* gene mutations in primary prostate tumors in patients. These data strongly support the hypothesis that the gene acts as a tumor suppressor. The original work of our laboratory identified a novel mechanism of growth regulation that involves allosteric regulation of c-Abl tyrosine kinase. This mechanism is novel and therefore is the subject of a patent application. Our mechanistic studies of primary prostate mutations using the LNCaP cell line as a model system suggest that loss of Abi1 function leads to dysregulated c-Abl kinase activity, enhanced cell proliferation and spreading, and subsequently to prostate tumorigenesis. Dysregulated c-Abl kinase activity has been implicated in various forms of leukemia, thus leading to us to hypothesize that prostate tumorigenesis may involve a similar mechanism. The potential role that Abi1/Hssh3bp1 may play in suppressing prostate tumor development has never been explored. Our novel Abi1/Hssh3bp1 conditional knock-out mouse model makes this possible. By breeding our model with other existing mouse models for prostate cancer (e.g., Pten model), we will also be able to study for the first time potential genetic interactions between Abi/Hssh3bp1 and other suppressor genes. Initial data from cell lacking the gene seem to support the hypothesis that Abi1/Hssh3bp1 acts as tumor suppressor. In addition we identified PI3-kinase pathway as candidate pathway that may work downstream of Abi1/Hssh3bp1. This pathway will be our focus in the next funding period.

References

Machida, K., C.M. Thompson, K. Dierck, K. Jablonowski, S. Karkkainen, B. Liu, H. Zhang, P.D. Nash, D.K. Newman, P. Nollau, T. Pawson, G.H. Renkema, K. Saksela, M.R. Schiller, D.G. Shin, and B.J. Mayer. 2007. High-throughput phosphotyrosine profiling using SH2 domains. *Mol Cell*. 26:899-915.

Macoska, J.A., J. Xu, D. Ziemnicka, T.S. Schwab, M.A. Rubin, and L. Kotula. 2001. Loss of expression of human spectrin src homology domain binding protein 1 is associated with 10p loss in human prostatic adenocarcinoma. *Neoplasia*. 3:99-104.

Xiong, X., P. Cui, S. Hossain, R. Xu, B. Warner, X. Guo, X. An, A.K. Debnath, D. Cowburn, and L. Kotula. 2008. Allosteric inhibition of the nonMyristoylated c-Abl tyrosine kinase by phosphopeptides derived from Abi1/Hssh3bp1. *Biochim Biophys Acta.* 1783:737-47.

Appendix

1. **Manuscript draft:** Dubielecka, P.M., Schloen, K.S., Xiong, X., Vedvyas, Y., Rottner, K., Stradal, T., and L. Kotula. Phenotypic Characterization of Cells Lacking Abi1/Hssh3bp1 Gene. *Manuscript under preparation.*

2. **Abi1/Hssh3bp1 phosphotyrosine SH2 domain screening document.**

Version 033109

Phenotypic Characterization of Cells Lacking Abi1/Hssh3bp1 Gene

Patrycja M. Dubielecka[1#], Kathrin Schloen[2#], Xiaoling Xiong[1], Yogindra Vedvyas[1], Klemens Rottner[3], Theresia Stradal[2] and Leszek Kotula[1]*

[1]Laboratory of Cell Signaling, New York Blood Center, New York, NY 10065

and

[2]Signaling and Motility and [3]Cytoskeleton Dynamics Group,

Helmholtz Institute for Infection Research, D-38124 Braunschweig, Germany

Running title: Phenotype of Abi1/Hssh3bp1 KO cells

Keywords: cell motility, actin cytoskeleton, Rho GTPases, cell growth, Abi1/Hssh3bp1

[#]These authors contributed equally to this work. Address correspondence to: Leszek Kotula, Laboratory of Cell Signaling, 310 E. 67th St., New York, NY 10065. Tel.: 212-570-3228; Fax: 212-570-3355; E-mail: lkotula@nybloodcenter.org.

Abstract/Summary of Progress

A substantial body of evidence indicates that Abi1/Hssh3bp1 plays a critical role in the regulation of the actin cytoskeleton and cell growth. However, detailed mechanisms of this regulation are not well defined. In order to further our understanding of Abi1/Hssh3bp1 function, we generated a conditional Abi1/Hssh3bp1 knockout (KO) mouse. Our initial analyses focused on phenotypic characterization of mouse embryonic fibroblasts. Following disruption of the Abi1/Hssh3bp1 gene through Cre recombinase-mediated deletion of exon 1, several MEF cell lines lacking a functional Abi1/Hssh3bp1 gene were obtained. Initial evaluation of actin cytoskeleton regulation in these cell lines indicated decreased dorsal ruffling but unchanged peripheral ruffling in comparison to control cells. Moreover, Abi1/Hssh3bp1 KO cells exhibited decreased migration rates and distances, but increased directional persistence in cell motility assays. Western blot analysis of Abi1/Hssh3bp1 KO cell lysates indicated decreased expression of the Wave 2 complex components Wave 2, Nap 1, and Sra1/PIR121. No decrease in Rac 1 expression or activity was observed in the KO cells, suggesting that either Rac 1 acts solely upstream of Abi1/Hssh3bp1, or that Rac1 regulation by Abi1 is compensated by unknown mechanisms.

In experiments involving cell growth regulation consistent with the tumor suppressor hypothesis, cells lacking functional Abi1/Hssh3bp1 gene exhibited enhanced proliferation rates. In addition we confirmed functionality of the Abi1/Hssh3bp1 gene loxP sites in vivo in mouse prostate tissue. Hence our conditional Abi1/Hssh3bp1 strain represents a novel and viable mouse model for molecular and tissue studies of Abi1/Hsshb3p1 gene and protein function.

Background/Introduction/Literature review

Understanding of actin cytoskeleton regulation is critical for our understanding of the molecular pathology of human developmental disease and cancer. It has become clear that the actin cytoskeleton plays an essential role in normal nervous system development (Scott and Olson, 2007), and in muscle development and function (Batchelor and Winder, 2006). Actin cytoskeleton aberrations are implicated in human developmental disease such as neural tube defects (Waes and Finnell, 2001). Most importantly, however, actin cytoskeleton dysregulation is associated with all stages of human cancer regardless of origin (Vega and Ridley, 2008). It is also becoming apparent that molecular processes regulating normal cell growth and proliferation, survival, and apoptosis must be coordinated with actin cytoskeleton regulatory processes to ensure proper tissue development and function. The need for detailed understanding of these processes is growing, as specific knowledge of molecular mechanisms underlying human cancer offers immediate diagnostic and treatment strategies (Druker, 2006), thus providing a basis for future personalized treatment of individuals (Mischel and Cloughesy, 2006).

Actin polymerization in cells is regulated by several mechanisms. Essential physiological processes such as cell migration, adhesion and endocytosis are all dependent on coordinated remodeling of the actin cytoskeleton, but the complexity of the mechanisms at play is just beginning to be appreciated (Niedergang and Chavrier, 2005), (Pollard and Borisy, 2003). The filaments that comprise the actin cytoskeleton are constantly turned over by polymerization/depolymerization cycles, although the dynamics of these processes may vary markedly depending on the structure or cell type. Nucleation of actin filaments is catalyzed by different types of enzymes, the most prominent of which include the Arp2/3-complex and members of the formin family of proteins (for reviews see (Faix and Grosse, 2006) & (Goley et al., 2006) These nucleation machines are regulated by additional proteins. In the case of the Arp2/3 complex, so called type I and type II nucleation promoting factors (NPFs) are essential intermediates that integrate and transduce incoming signals (Stradal et al., 2004) (Welch and Mullins,

2002). The WASP- and WAVE-subfamilies constitute the most prominent NPFs and have received significant attention in recent years (Stradal and Scita, 2006), not only because they constitute key signaling nodes that connect activation signals from the Rho family of small GTPases with the actin polymerization machineries, but also because the N-WASP and Arp2/3 complexes have emerged as frequent targets for viral or bacterial pathogens that usurp the host actin cytoskeleton for their needs (Gouin et al., 2005) (Patel and Galan, 2005) (Rottner et al., 2005). Much less is known regarding cellular functions exerted by the formin family of proteins, which are just beginning to be understood. The formin family proteins also act directly downstream of Rho-GTPases; however, the molecular mechanisms of actin nucleation/polymerization mediated by Rho-GTPases are entirely different than the mechanisms mediated by N-WASP and Arp2/3 complexes. In contrast to the Arp2/3 complex, which generates new actin filaments through the formation of branches, formins generate linear actin filaments, such as those of yeast actin cables, stress fibers, and filopodia (Zigmond, 2004). Moreover, whereas the Arp2/3 complex is not known to contribute to the elongation of filaments once they are formed, formins reside on the fast growing filament plus end and catalyze elongation until the signal ceases (Kovar and Pollard, 2004). Most of the 20 Rho family GTPases (Ridley, 2006) in mammals have been linked in one way or another to reorganizations of the actin cytoskeleton (Aspenstrom, 2004), although the vast majority of studies still refer to the function of the best-studied family members Cdc42, Rac1, and RhoA, respectively, as triggering the formation of filopodia, lamellipodia, and contractile structures such as stress fibers (Hall, 1998). Rac and Cdc42 subfamily members are important stimulatory switches driving the formation of lamellipodia and filopodia, although the precise signaling pathways from a given GTPase to the respective actin polymerization machinery are far from fully elucidated.

Abi1/Hssh3bp1 is a component of Wave complex that regulates lamellipodia formation. Lamellipodia are flat, sheet-like membrane protrusions filled with a mesh of filamentous actin continuously polymerizing at their plus ends, all of which point towards the cell edge. Our understanding of the molecular mechanisms that underlie lamellipodium protrusion and membrane ruffling has progressed significantly in the last few years.

Recent work has shown that lamellipodium formation, at least downstream of Rac1, requires a protein assembly termed WAVE-complex. In tissue culture cells, this complex consists of ubiquitously expressed variants of 5 polypeptides, specifically, the Rac1-associated protein 1 (Sra-1), Nck- associated protein 1 (Nap1), Abl interactor-1 (Abi-1, Hssh3bp1) and WAVE2, as well as a 9 kD-peptide called Brck-1 or HSPC300 (Stradal et al., 2004) (Takenawa and Suetsugu, 2007) and references therein. Except for Brck-1, which is a single copy gene, each of these proteins is member of a protein family comprised of two or three genes in mammals: Sra-1 and PIR121 (also known as Cyfip1 and Cyfip2); Nap1 and Hem1; Abi-1, Abi-2 and NESH (also called Abi-3); and WAVE1, WAVE2 and WAVE3. Most of the isoforms have been shown to assemble into WAVE-complexes in comparable fashion to the aforementioned variants (e.g. (Stovold et al., 2005) , but isoform-specific functions within (Suetsugu et al., 2003), or independent of, differentially formed WAVE complexes were also suggested, e.g., (Innocenti et al., 2005). Downregulation by RNA interference of any of the components except Brck-1 completely abolishes lamellipodium protrusion and membrane ruffling (Innocenti et al., 2004), (Steffen et al., 2004) These and other data gave rise to a model in which Rac1 activation initiates a sequence of events leading to WAVE-complex activation and recruitment to the cell periphery, eventually leading to WAVE-mediated activation of the Arp2/3-complex, and consequent actin assembly (reviewed in (Stradal and Scita, 2006). This model is strengthened by more recent reports, firstly by the demonstration that RNAi-mediated suppression of Arp2/3-complex expression also abrogates lamellipodium protrusion (Steffen et al., 2004) , and secondly by the observation of defects in ruffling and lamellipodium protrusion in fibroblasts following transient genetic removal of Rac1. This highlights a crucial role for Rac1 in WAVE-complex activation. In the current proposed research, using cells isolated from the first genetic knockout of Abi1/Hssh3bp1 as a model system, we will define this regulation. It remains to be established whether or not Rac1 is the only small GTPase that directly signals activation of the WAVE-complex. Mammals express additional, highly homologous Rac proteins, all of which are capable of lamellipodium induction when over-expressed as constitutively active variants in fibroblastic cells (Aspenstrom, 2004). Among these are Rac2, the expression of which is restricted to the hematopoietic system, and Rac3, which is more widely expressed.

Although Rac2 has turned out be an important regulator of actin reorganization in different cells of hematopoietic origin (reviewed in (Ridley, 2006), it is not known how this GTPase signals actin assembly. Although our research focuses on Abi1/Hssh3bp1-Rac1 function, hypotheses regarding Rac2 or Rac3 will be established based on the available Rac1 data.

Abi1/Hssh3bp1 was identified by our group as human spectrin SH3 domain binding protein. Spectrin is an actin binding protein and is the predominant component of the multi-dimensional protein network of the membrane skeleton underlying the lipid bilayer of red cells. Mutations that affect interactions of membrane skeleton proteins cause increased fragility and shortened lifespan of erythrocytes leading to hereditary anemias (reviewed in (Joiner et al., 1995) and (Gallagher and Ehrenkranz, 1993)). Spectrin and many of its interacting proteins, which were first identified in red cells, have isoforms expressed in non-erythroid cells, but the structure and regulatory processes of the non-erythroid membrane skeleton are less well understood**.** Functional differences between the membranes of erythroid and non-erythroid cells argue against the simple erythroid model of the membrane skeleton. Major differences between the erythroid model and other cells include differences in the expression of spectrin and ankyrin isoforms, interactions of spectrin and ankyrin with additional proteins, localization of spectrin in the cytoplasm as well as in the plasma membrane, and the potential for dramatic rearrangements of spectrin's cellular location. These differences may account for specialized functions of the non-erythroid membrane skeleton in different cell types (Goodman et al., 1995), (De Matteis and Morrow, 2000) (Bennett and Baines, 2001). We have a long-standing interest in spectrin and membrane skeleton regulation. We cloned the alpha I spectrin gene (Kotula et al., 1991), functionally characterized the spectrin region involved in hereditary anemia (Kotula et al., 1993) and originally identified human spectrin SH3 domain binding protein or Hssh3bp1 (Ziemnicka-Kotula et al., 1998) (original HUGO symbol SSH3BP1). We demonstrated that Hssh3bp1 binds Abl tyrosine kinase and we mapped the specific region of Hssh3bp1 responsible for this interaction. On the basis of our findings we postulate that Hssh3bp1 may target tyrosine kinases such

as Abl to the membrane skeleton through binding to the spectrin SH3 domain. In this scenario, spectrin may provide a scaffold for signal transduction proteins and in this way play a role in the signal transduction processes. Our current research extends this hypothesis further to identification of mechanisms of actin cytoskeleton and cell growth regulation by Abi1/Hssh3bp1 using cells lacking this protein.

Abi1/Hssh3bp1 regulates Abl kinase activity. Hssh3bp1 (Ziemnicka-Kotula et al., 1998) is a human ortholog of mouse Abi1 (Shi et al., 1995). E3b1, which is identical to isoform 2 of Hssh3bp1 (Ziemnicka-Kotula et al., 1998), was identified independently by another group as the eps8 (epidermal growth factor substrate 8) SH3 domain binding protein (Biesova et al., 1997). Abi1 and Abi2 were identified as proteins binding to Abl kinase (Dai and Pendergast, 1995; Shi et al., 1995). Initial work, including our own, on Abi1 and Abi2 suggested that these proteins might play a role in negative regulation of Abl kinase (Dai and Pendergast, 1995; Ikeguchi et al., 2001; Macoska et al., 2001). More recently, we demonstrated direct involvement of Abi1/Hssh3bp1 in regulation of Abl kinase activity (Xiong et al., 2008). Using peptides derived from Abi1 we showed that Abi1 inhibits c-Abl tyrosine kinase activity *in vitro* through binding to Abl SH3 and SH2 domains. Moreover stable expression of Abi1 in the Abi1-deficient human prostate cell line, LNCaP, inhibited pervanadate-induced Abl kinase activity only when intact SH3 and SH2 domain binding sequences were present (Xiong et al., 2008). Discovery of this regulation has important implications, not only for our basic understanding of kinase regulation, but also for our understanding of the clinically relevant BCR-Abl kinase that underlies chronic myelogenous leukemia (CML). Mutations in Abl SH3 and SH2 domains thought to confer Gleevec resistance have been found in a tissue culture model for identifying Gleevec-resistant mutations (Azam et al., 2003). Increasing experimental evidence suggests that Abi1 is important for BCR-Abl signaling leading to experimental leukemia in mice (Yu et al., 2008). Therefore it is critical to develop a detailed understanding of the molecular regulation of Abl kinase by Abi1/Hssh3bp1. The Abi1/Hssh3bp1 KO mouse model and associated cell lines lacking a functional Abi1/Hssh3bp1 gene that we have developed will permit further analysis of the role of Abi1/Hssh3bp1 in Abl kinase regulation.

Abi1/Hssh3bp1 is a candidate tumor suppressor frequently mutated in prostate cancer. Our original localization of the Abi1/Hssh3bp1 gene to 10p11.2 suggested its possible involvement in prostate cancer because as much as 55% of the loss of heterozygosity (LOH) observed in prostate cancer occurs at 10p (reviewed in (Ittmann, 1998; Narla et al., 2003; Yoshida et al., 1998). In pilot studies we evaluated Abi1/Hsshb3p1 expression by immunocytochemistry in 17 primary prostate tumor cases. These cases were comprised of paired normal and malignant prostate tissue specimens. We found that 4 out of 6 tumors with 10p deletion involving two microsatellite markers, D10S89 and D10S111, did not express Abi1/Hssh3bp1. Additionally, 5 of 11 tumors that were diploid for D10S89 and D10S111 failed to express Abi1/Hssh3bp1. Although this study involved only a small number of cases, the data suggested that Abi1/Hsshb3p1 may act as a tumor suppressor that is inactivated in some prostate tumors (Macoska et al., 2001). Prostate-specific disruption of the Abi1/Hssh3bp1 gene in the conditional Abi1/Hssh3bp1 KO mouse will provide proof-of-principle evidence for the role of Abi1/Hssh3bp1 in prostate cancer. Subsequently, the Abi1/Hssh3bp1 KO mouse can be used to determine if Abi1/Hssh3bp1 plays a role in tumorigenic growth in other tissues.

Production of the conditional Abi1/Hssh3bp1 KO mouse to determine the physiological role of the gene in an in vivo system. Identification of inactivating mutations in primary human prostate tumors suggests that Abi1//Hssh3bp1 carries tumor suppressor function. Thus, we hypothesize that prostate-specific disruption of the mouse ortholog leads to prostate tumorigenesis. Recapitulation of the disease process in the mouse model will provide proof of principle for the role of Abi1/Hssh3bp1 in prostate cancer. In addition, no cell culture model of cells lacking Abi1/Hssh3bp1 following genetic knockout of the gene is available. These points were the major rationale behind the decision to produce the Abi1/Hssh3bp1 KO mouse. The decision was made to produce conditional and not conventional KO for two reasons: the conventional Wave 2 KO mouse is embryonic lethal (Yamazaki et al., 2003; Yan et al., 2003), thus suggesting that conventional disruption of Abi1/Hssh3bp1 in the mouse may be also lethal, and secondly, conditional

KO models are better cancer disease models, as tissue specific and developmental stage-specific disruption of genes can be achieved.

Possible functions of Abi1/Hssh3bp1. We are just beginning to appreciate the physiological role of Abi1/Hssh3bp1. For example, the *Xenopus laevis* homolog of Abi1/Hsshb3p1, *xlan4*, was demonstrated to be critical for CNS development, and this may be true for another Abi1/Hssh3bp1 related protein, Abi2, in mice (Courtney et al., 2000). Further work on Abi2 using mouse embryonic fibroblasts obtained from the Abi2 knockout mouse indicates a critical function of Abi2 in cell-cell adhesion, cell migration, and tissue morphogenesis. The Abi2 KO mouse exhibits severe short and long-term memory loss thought to be due to an observed deficiency in dendritic spine and adherens junction formation, and abnormal cell-cell communication. All of these findings are consistent with a role for Abi2 in the regulation of cytoskeletal dynamics. Cytoskeletal effects of Abi1 function have been confirmed in Dictyostelium Abi KO cells, and, in addition, this study identified the role of Abi in cytokinesis (Pollitt and Insall, 2008). Dictyostelium has only one Abi gene; thus it offers no specific conclusion for mammalian roles of Abi1 or 2 genes. In 2004, Echarri et al (Echarri et al., 2004) reported cells from a heterozygous, conventional Abi1 KO mouse, but no information has been reported addressing Abi1/Hssh3bp1 function in a homozygous knockout of Abi1/Hssh3bp1 at the cellular or tissue level. Therefore, our Abi1/Hssh3bp1 conditional KO mouse provides the critical model for such studies.

The physiological significance of macropinocytosis is not well defined. Macropinocytosis is characterized by extensive plasma membrane reorganization initiated by membrane ruffling and formation of an external macropinocytic structure, which is subsequently enclosed and internalized as a macropinosome. Macropinosomes may be distinguished from other forms of pinocytic vesicles by their lack of coating structures, heterogeneity, and larger and variable size (0.2-2.0 μm) (Amyere et al., 2002; Nichols and Lippincott-Schwartz, 2001; Swanson and Watts, 1995). Many extracellular fluid-soluble molecules and large particles such as viruses, bacteria, and apoptotic fragments can be internalized by macropinocytosis (Fiorentini et al., 2003; Krysko et al.,

2006; Meier and Greber, 2004; Norbury, 2006). Macropinocytosis is involved in numerous processes including nutrient uptake and degradation (Cardelli, 2001), down-regulation of plasma membrane receptors following ligand binding (Jones et al., 2006), and antigen processing and maturation of dendritic cells (Norbury, 2006; Watts et al., 1989). In macrophage, epithelial, tumor, and other cell lines, macropinocytic uptake increases upon activation of growth factor receptors (Berfield et al., 2006; Bryant et al., 2007; Davies and Ross, 1978; Haigler et al., 1979; Hewlett et al., 1994; Miyata et al., 1988; Offenhauser et al., 2004; Racoosin and Swanson, 1992). Treatment with mitogenic agents such as phorbol esters and diacylglycerol also result in enhanced macropinocytosis (Seastone et al., 1999; West et al., 1989; Zhao et al., 2006). Despite significant progress in understanding macropinocytosis, many questions remain. One important objective of the current research regarding the regulation of macropinocytosis will be to determine the mechanism by which growth factor and mitogenic signaling is coordinated with actin cytoskeleton reorganization.

Involvement of the actin cytoskeleton in macropinocytosis is well established. Each step of macropinocytosis, from ruffle formation to engulfment of a ruffle into a macropinosome, is thought to be regulated by multiple actin polymerization/depolymerization events (Falcone et al., 2006; Swanson and Watts, 1995). Abi1/Hssh3bp1 (Biesova et al., 1997; Shi et al., 1995; Ziemnicka-Kotula et al., 1998) is a key component of several intrinsic complexes that regulate actin cytoskeletal remodeling near the plasma membrane (Ibarra et al., 2005). Overexpression of Abi/Hssh3bp1 in NIH 3T3 cells inhibits macropinocytic uptake of fluorescent, water-soluble markers (Xu et al., 2000). Numerous isoforms of Abi1/Hssh3bp1 exist in mammalian cells (Ikeguchi et al., 2001; Stradal et al., 2001; Ziemnicka-Kotula et al., 1998) providing a potential diversity of Abi1/Hssh3bp1-actin regulatory complexes, which suggests the possibility of multiple mechanisms through which Abi1/Hssh3bp1 might regulate macropinocytosis. Critical questions regarding the role of Abi1/Hssh3bp1 can now be addressed in cells lacking the Abi1/Hssh3bp1 gene.

Studies of the past decade revealed that Abi1/Hssh3bp1 participates in several multi-protein complexes that regulate the dynamics of actin polymerization (Stradal and Scita, 2006). Molecules that have been proposed to form complexes with Abi1/Hssh3bp1 include Eps8-Sos1 (Innocenti et al., 2003; Scita et al., 1999), N-Wasp (Bogdan et al., 2005; Innocenti et al., 2005), and Wave complex (Gautreau et al., 2004; Innocenti et al., 2004; Steffen et al., 2004) including both Wave1 and Wave2. Each of these actin regulatory complexes involves a different mechanism, although at least two of these mechanisms converge directly on Rac1 function. The first, Eps8-Sos1-Abi1/Hssh3bp1, was proposed to act as a Rac1 guanine exchange factor (GEF) which activated Rac1 independent of Ras signaling (Scita et al., 1999). The second, Abi1/Hssh3bp1-containing Wave2 complex has been directly linked to the effect of Rac1 on increased actin polymerization at the plasma membrane at the site of control of lamellipodia formation (Innocenti et al., 2004; Steffen et al., 2004). Mechanistically, it is hypothesized that active Rac1 targets the Wave2 complex to the plasma membrane where Rac1 is responsible for activation of Wave2/Arp2/3-dependent actin polymerization (Steffen et al., 2004). Increased actin polymerization near the plasma membrane, which is associated with increased macropinocytic uptake, may explain the postulated role of Rac1 in regulation of macropinocytosis. In this regard it has been demonstrated that a dominant negative Rac1 (Rac1-T17N) downregulates fluid uptake of dextrans, but that constitutively active Rac1 (Rac1-Q61L) upregulates the process (Ridley et al., 1992; West et al., 2000). Rac1 does not directly interact with Wave, but instead binds to the Nap1-binding protein Sra-1, both of which in turn associate with Abi1 (Gautreau et al., 2004). Abi1 interacts with Wave2 and couples it to Abl kinase activity following cell stimulation, thus promoting Wave2 phosphorylation (Leng et al., 2005). Tyrosine phosphorylation may regulate Wave complex activity either by regulating conformation of the complex as suggested (Leng et al., 2005), or by regulating interactions among components of the complex such as Abi1 and Abl kinase (Xiong et al., 2008). Wave complex activity may also be modulated by its interaction with PIP3 and PIP3-mediated membrane recruitment (Oikawa et al., 2004; Suetsugu et al., 2006), or possibly through independent IRSp53-mediated binding to both Cdc42 and Rac1 (Abou-Kheir et al., 2008; Funato et al., 2004; Suetsugu et al., 2006).

Abi1/Hssh3bp1 may also regulate macropinocytosis through its adaptor function by regulating or localizing various kinase activities that are important for the process. Interaction of Abi1 with the p85 regulatory subunit of PI3-kinase targets the kinase activity to membrane ruffles (Innocenti et al., 2003). PI3-kinase activity was originally proposed to play a role in the closure of immature membrane ruffles to produce a macropinosome (Araki et al., 2007; Araki et al., 1996). Recent studies supporting the importance of PI3 kinase and PIP signaling in the process (Amyere et al., 2000) suggest that macropinosome maturation involves subsequent PIP2-, PIP3-, and Rab5-enriched stages, all involving signaling downstream from Ras (Porat-Shliom et al., 2008), thus confirming the original identification of Ras involvement in macropinocytosis (Bar-Sagi and Feramisco, 1986). Abi1/Hssh3bp1 regulation of macropinocytosis downstream from growth factor receptor-signaling may involve nonreceptor tyrosine signaling that is independent of Ras. That tyrosine kinase signaling is critical for macropinocytosis is suggested by the fact that active Src accumulates in membrane ruffles (Veithen et al., 1996). Other tyrosine kinases, such as Arg and Abl kinases, that have been shown to modulate membrane ruffling (Boyle et al., 2007; Jin and Wang, 2007) provide a link between mitogenic signaling downstream of growth factor receptors and actin cytoskeleton regulation. Abi1/Hssh3bp1 is probably the major transmitter of Abl kinase-dependent effects on the actin cytoskeleton through Arp2/3-dependent actin polymerization as discussed above. The serine-threonine kinase, PAK2, may regulate interaction of Abi proteins with Abl through phosphorylation of the Abi-SH3 domain-binding site on Abl (Jung et al., 2008), providing yet another potential mechanism for the well established role of PAK proteins in macropinocytosis (Dharmawardhane et al., 2000; Liberali et al., 2008).

We originally demonstrated expression of multiple isoforms of Abi1/Hssh3bp1 (Ziemnicka-Kotula et al., 1998) although the functional significance of the various isoforms has not been addressed. The diversity of Abi1/Hssh3bp1-dependent signaling coupled with the variety of adaptor functions suggested the possibility that different Abi1/Hssh3bp1 isoforms differentially mediate specific effects of Abi1/Hssh3bp1

regulatory activities in macropinocytosis. In our paper (Dubielecka et al, in revision), we demonstrated that expression of isoform 2 and isoform 3 have opposing effects on Alexa Fluor 647 uptake in Ab1/Hssh3bp1-deficient LNCaP (Macoska et al., 2001) cell lines stably transfected with Abi1/Hssh3bp1 isoforms. In addition, expression of isoform 2 and 3 produce different effects on actin cytoskeleton dynamics resulting in changes in cell spreading activity, and in differences in cell morphology. We hypothesize that these differences are due to the differential binding of active Rac1 to Abi1/Hssh3bp1 isoforms or isoform-specific complexes, thus suggesting the possibility of differential regulation of Rac1 activation by Abi1 isoforms. More comprehensive analysis of Abi1/Hsshb3p1 will be facilitated by use of Abi1/Hssh3bp1 KO cell lines now available in our laboratory.

Abi1/Hssh3bp1 may control cell growth through Abl-PI3K-Akt pathway. Akt, also known as protein kinase B, acts as a tumor-promoter by inhibiting apoptosis due to specific activation of mTOR1 (Skeen et al., 2006). Akt is activated by the action of growth factor receptors leading to enhanced function of PI3 kinase and PKD-dependent phosphorylation of Akt on tyrosine 308. Decreased Akt phosphorylation has been recently reported in breast cancer cell lines consequent to siRNA-dependent down regulation of Abi1 (Wang et al., 2007). These studies, therefore, suggest that the PI3K-Akt pathway is downregulated upon siRNA knockdown of Abi1/Hssh3bp1. PI-3 kinase has been linked to Abl kinase regulation for almost two decades without clear elucidation of the mechanism (Kharas and Fruman, 2005; Varticovski et al., 1991). Availability of Abi1/Hsshb3p1 KO cell lines will permit detailed analysis of the PI3K-Akt pathway in Abi1/Hsshb3p1 KO cells in relationship to Abl kinase regulation. Considering current drug development efforts that focus on Abl and Akt-mTOR inhibitors (Abraham and Gibbons, 2007; Druker, 2006), examination of this hypothesis is of great importance for our understanding of molecular mechanisms leading to human cancer.

Materials and Methods

Construction of the targeting vector for the mouse Abi1 gene. The murine Abi1 gene (gene accession number NM_007380), and the human gene orthologue ABI1/SSH3BP1 (NM_005470) was targeted. An approximately 11.8kb region used to construct the targeting vector was first subcloned from a positively identified BAC clone using a homologous recombination-based technique. The region was designed such that the short homology arm (SA) extends 1.9 kb 3' to exon 1. The long homology arm (LA) ends on the 5' side of exon 1 and is approximately 9kb long. The single loxP site is inserted 5' to exon 1, and the loxP-flanked Neo cassette is inserted 3' to exon 1. The target region is 0.9kb and includes exon 1. The targeting vector was confirmed by restriction analysis after each modification step and by sequencing using specific primers.

Transfection and isolation of 129SvEv Embryonic Stem (ES) Cells. The conditional targeting construct was transfected into 129SvEv embryonic stem (ES) cells, and approximately 300 antibiotic-resistant colonies were selected. After in vitro expansion, aliquots of cells were lysed, DNA was extracted, purified, and dried into 96-well tissue culture plates. The 96-well plates of DNA isolated from the homologous recombinant clones were screened using a PCR-based strategy utilizing PCR primers located in both the short homology arm and within the Neo cassette. Positive clones were then submitted for sequencing to confirm proper integration of all loxP (Sauer and Henderson, 1988; Sternberg and Hamilton, 1981) and frt (Sadowski, 1995) sites, and then finally expanded into cultured ES cells.

Generation of transgenic mice. Two positive ES cells of clones (1-2D3 and 1-3D1) were microinjected into C57BL/6 blastocysts, which were then implanted in the uteri of pseudo-pregnant females. The pseudo-pregnant female mice then gave birth to offspring, and upon reaching four (4) weeks of age, chimerism of pups was analyzed by coat color observation. Five (5) males of at least 90% agouti chimerism were obtained. At six (6) weeks of age, chimeric mice were harem-mated with C57BL/6 female mice for the

production of F1 heterozygous offspring. Both F1 heterozygous male and female mice were obtained and confirmed by genotyping.

Breeding of Abi1/Hssh3bp1 floxed mice. Mice heterozygous for the recombinant Abi1/Hssh3bp1 allele containing neomycin gene, frt sites and loxP sites were bred with the "frt deletor" strain 129S4/SvJaeSorGt(ROSA)26Sortm1(FLP1)Dym/J (Jackson Laboratories, Inc. stock number 003946). Flipase-mediated deletion of the neomycin gene from the recombinant gene cassette was confirmed by genotyping with specific primers. Heterozygous Abi1/Hssh3bp1 animals Abi1/Hssh3bp1 ($loxP^{+}$/wt) also called Abi1/Hssh3bp1 (fl/+) or (floxed/+) were subsequently bred to obtain homozygous Abi1/Hssh3bp1 (fl/fl) mice. Mouse embryonic fibroblast (MEF) cell lines were subsequently obtained from these mice.

Establishment of Abi1/Hssh3bp1 knockout cell lines. Isolation of primary mouse embryonic fibroblasts (day 13.5) was performed as described (Abbondanzo et al., 1993) with some modification (Nagy, 2003). MEF cell lines were immortalized by retroviral transduction of the SV40 large T antigen (Jat and Sharp, 1986) Following genotype confirmation, homozygous Abi1/Hssh3bp1 (fl/fl) MEF cell lines (parental MEF # 3 and parental MEF # 8) were used to obtain syngeneic cell lines in vitro (i.e. for in vitro genetic knockout experiments). The Abi1/Hssh3bp1 (fl/fl) cell lines were either transiently transfected with a Cre recombinase encoding plasmid in order to remove the floxed alleles, or with a control EGFP plasmid expressing puromycin. Both plasmids carried the puromycin resistance cassette. For transfection FuGene6 reagent was used according to the manual (Roche). Transfection medium was replaced after 24 hours by normal medium supplemented with 5μg/ml puromycin. Cells were cultured with puromycin for the following six days (the appropriate puromycin concentration was achieved by performing a killing curve). Cell lines were then cultured under normal conditions as described above. Single clones were obtained by limiting dilution subcloning. For each Abi1/Hssh3bp1 precursor cell line at least 10 individual Abi1 KO cell clones were established. The effective removal of the Abi1 floxed alleles in cells

transfected with the Cre recombinase encoding plasmid was confirmed by PCR, by evaluation of protein expression levels, and by RNA-array analysis.

Tissue culture media, antibiotics and transfection reagents. MEF cell lines were maintained in DMEM, 10 % fetal calf serum (FCS), non essential amino acids (NEAA), L-glutamine and sodium pyruvate, at 37 °C and 7.5 % CO_2. The following culture media were from Invitrogen: DMEM (high glucose), Cat. 41965-039; Non-essential amino acids (NEAA), Cat. 11140-035; L-Glutamine, Cat. 25030-024; and Sodium pyruvate. Fetal calf serum (FCS) was from Sigma. pCre-Pac was as described (Taniguchi et al., 1998); pEGFP-N3 was from Clontech. Puromycin was from Sigma. FuGene6 was from Roche.

PCR genotyping of Abi1/Hssh3bp1 strains. For confirming the targeted allele (2.408kb) containing the neomycin gene, frt sites and 3' and internal loxP sites (neo+frt+loxP+), in chimeras and in the F1, the following primers were used: Forward primer, LAN1: 5'- CCA GAG GCC ACT TGT GTA GC -3'; reverse primer A2: 5'- CTG GAA GCT GAC AAG AGG ATA G -3'. For the wild type allele (WT) (625bp) the following primers were used: forward primer, WT1: 5'- GAT GCC GCT CCC CGC AGC CTG C -3'; reverse primer, SG1: 5'- CAC TCT CCG CAC TCG ATT AGG -3'.

PCR-based detection of Abi1 floxed allele or exon 1 deletion by Cre recombinase-mediated recombination. We used several primer pairs to confirm functionality of loxP sites and to determine the Abi1/Hssh3bp1 exon 1 deletion due to expression of Cre recombinase. For the floxed allele (Abi1(fl)) and exon 1 deleted allele (Abi1(-)) the following primers were used: Primer pair: mAbi1loxP35' and FlankNeo13': Forward primer, mAbi1loxP35': 5' - AAT AAT TTA ATA GTT CTG GTG ATA TGA CAG C - 3'; Reverse primer, FlankNeo13': 5' - GGG CAG ACG GCG AGA AGC AGA G - 3'. Resulting PCR fragments are the following: recombinant floxed band @ 1.903 kb, wild type band @ 1.662 kb; deleted allele @ 0.841 kb. For the primer pair: DL75' and FlankNeo13'; forward primer, DL75'**:** 5' - TAG GGT ACA AAT TAT CCT TGC TTC - 3'; reverse primer, FlankNeo13': 5' - GGG CAG ACG GCG AGA AGC AGA G - 3'.

Resulting PCR fragments: recombinant floxed @ 1.334 kb; wild type @ 1.093 kb; deleted allele @ 0.272 kb. For primer pair DL75' and Neogene13': forward primer, DL75': 5'- TAG GGT ACA AAT TAT CCT TGC TTC - 3'; reverse primer, Neogene13'; 5' - GTG TTG ACG AGG CGT CCG AAG AAC G- 3'. Resulting PCR fragments are the following: recombinant floxed band @ 1.233 kb; deleted allele @ 0.171 kb. No wild type band is observed with this primer set as this pair only works on the recombinant sequence. Due to high GC content of the exon 1 region for PCR genotyping reactions Clontech Advantage GC or Advantage HF PCR reaction kits (Clontech Laboratories, Inc., Mountain View, CA) 9 were used with addition of GC melting reagent.

DNA isolation from mouse tails or tissue was performed using Charge Switch gDNA Mini Tissue kit (Cat. CS11204) (Invitrogen, Carlsbad, CA). MEF cell DNA was prepared using QIAamp (51304) (Qiagen, Valencia, CA).

Quantification of cell morphologies in Abi1 expressing and Abi1 knockout cell lines in response to PDGF. Abi1 control (# 3; # 8) and Abi1-deficient (# 3-6, # 3-11; # 8-7, # 8-11) cell lines were grown on glass-coverslips, serum starved in DMEM for 16-18 h followed by treatment with PDGF (10 ng/mL) in DMEM for five minutes at 37°C. Cells were fixed (4 % PFA in 1 x PBS; 20 min at RT), extracted (0.1 % Triton in 4 % PFA; 1 min at RT) and treated with fluorescently-labelled phalloidin (in PBS; 45 min at RT) to stain F-actin. Different cell morphologies observed upon PDGF addition were classified according to the following categories: with ruffles, without ruffles, or with ambiguous cell morphology. At least 100 cells were analyzed and categorized for each condition. Platelet-derived growth factor-BB human was from Sigma, (P3201); Alexa Fluor 594 Phalloidin was from Molecular Probes (Invitrogen, 41A2-2).

Abi1 immunostaining in Abi1 control and -deficient cells after PDGF-stimulation. Abi1 control (# 3) and Abi1-deficient (# 3-11) cell lines were grown on glass-coverslips, serum starved in DMEM for 16-18 h followed by treatment with DMEM containing PDGF (10 ng/mL) for five minutes at 37°C. Cells were fixed (4 % PFA in 1 x PBS; 20 min at RT), extracted (0.1 % Triton in 4 % PFA; 1 min at RT) and stained with the

respective antibodies (60 min at RT) as indicated. Subsequently, cells were treated with the appropriate secondary antibody and fluorescently-labelled phalloidin (in 1 % BSA in PBS; 45 min at RT) to stain F-actin. Monoclonal antibodies used here either recognized both Abi1 and Abi2 (W8.3) or Abi1 (4E2) (Ziemnicka-Kotula et al., 1998) specifically. Monoclonal Abi1/2 antibody W8.3 was kind a gift from Giorgio Scita (IFOM, Milan, Italy). Secondary antibodies were goat anti-mouse Alexa Fluor 488, (Invitrogen - Molecular Probes, A11001) and Alexa Fluor 594 Phalloidin (Invitrogen -Molecular Probes, 41A2-2).

Antibodies to Wave complex components. Polyclonal antibodies to Wave 2, Sra 1, Nap1, Abi1/Hssh3bp1 (E3b1) were as described (Steffen et al., 2004). Mouse monoclonal anti-Rac1 antibody was from Cytoskeleton.

Rac activity assay. Rac activation assays were performed using the G-LISA kit from Cytoskeleton Inc. (Denver, CO). Abi1 control (# 3) and Abi1-deficient (# 3-6; # 3-11) cell lines were seeded in 10 cm tissue culture dishes. On the second day after seeding, cells were serum-starved for 16-18 h followed by mock treatment with DMEM or by treatment with DMEM containing PDGF (10ng/mL) for five minutes at 37 °C. The assay was performed according to the G-LISA manual.

Western blotting and immunoprecipitations were performed as described (Xu et al., 2000). Immunoprecipitates were washed extensively with buffer containing 0.1% Triton X-100, 20 mM HEPES, 50 mM NaCl, and protease inhibitors. Samples were prepared and analyzed by Western blotting as described (Ziemnicka-Kotula et al., 1998) except that NUPAGE gels (Invitrogen, Carlsbad, CA) were used. Antibodies to Abi1/Hssh3bp1 7B6 (Xiong et al., 2008), 4E2 (Ziemnicka-Kotula et al., 1998) were used for evaluation of Abi1/Hssh3bp1 levels. For general evaluation of protein levels in total cellular lysates gels were stained using GelCode Blue (Thermo Fisher Scientific, Waltham, MA).

Analysis of cell motility in cells lacking Abi1/Hssh3bp1. For random migration analysis, cells were seeded in 6-well plates at a density of 10^4 cells/well in regular growth

medium, and placed in a temperature- and CO2-controlled microscope chamber (Axiovert 200, Carl Zeiss, Microimaging Inc.). Time lapse recording started 6 hours after plating. Images were collected with a 10x objective at 15-minutes intervals over an 8 hour period, using a AxioCam MRm camera (Zeiss) and Axiovision software. Motility parameters including migration path, distance, rate and directional persistence were obtained from time-lapse movies. To track the migration path of individual cells, cells were manually located in each frame using ImageJ software (NIH ImageJ, software Version 1.41n); nuclei were used as geographical centers for tracking. The migration paths were expressed as graphs (Microsoft Office Excel 2003). The rates of cell migration were calculated as a ratio of the total length of migration paths and the duration of migration. Migration distances were determined as the net translocation during an 8-hour period. Directional persistence was calculated as a ratio of the direct distance during an 8-hour period and the total length of the migration path. **For wound-healing migration assay**, cells were seeded in 6-well plates at a density of 1×10^6 cells/well in regular growth medium. After 6 hours, the confluent monolayer of cells was scratched with a fine pipette tip, and migration was visualized by time-lapse imaging as described above. The rate of wound closure was determined by measuring the area not covered by cells per unit of time. Each assay was repeated at least four times.

Results and Discussion

Design and construction of the targeting vector. The goal in designing the targeting vector was to achieve disruption of Abi1/Hssh3bp1 gene expression by Cre-recombinase mediated deletion of Abi1/Hssh3bp1 exon 1 including the start codon downstream of the Kozak consensus sequence. Hence, the design of the Abi1/Hssh3bp1 targeting vector included placement of loxP sites around exon 1. The neomycin gene cassette was placed upstream of the 3' loxP site. The neomycin gene, including the third or internal loxP site, was placed between two frt sites for flp recombinase-mediated deletion (Fig. 1A).

Mouse breeding to obtain Abi1/Hssh3bp1 floxed mouse. Following successful breeding of Abi1/Hssh3bp1 chimeric mice, the germline transmission of the modified recombinant Abi1/Hssh3bp1 allele (containing the neomycin gene, frt and loxP sequences) was achieved and subsequently led to production of F1 strain. However, the homozygous strain, i.e. the strain containing two copies of the recombinant Abi1/Hssh3bp1 allele with all initial elements could not be obtained either at the F2 stage or in subsequent progeny, hence the recombinant allele transmission was maintained at the heterozygous stage. Subsequent breeding of the Abi1/Hssh3bp1 (loxP+/frt+/Neo+)/wt strain with the "frt deletor" strain led to removal of the neomycin gene, resulting initially in the heterozygous Abi1/Hssh3bp1 (fl/+) strain (Fig. 1B), which was then inbred to generate the homozygous Abi1/Hssh3bp1 (fl/fl) strain. The sequence of the floxed allele following flp-mediated recombination resulting in removal of neomycin gene is presented in Fig. 1C.

Isolation and immortalization of mouse embryonic fibroblasts (MEF cells) from Abi1/Hssh3bp1 floxed animals. Following isolation of primary mouse embryonic fibroblasts (MEF) as described in Material and Methods, cells were genotyped by PCR (Fig. 2A). Several MEF cell lines were randomly selected. These included cell lines expressing wild type Abi1/Hssh3bp1 as well as lines expressing the desired homozygous floxed Abi1/Hssh3bp1 gene (Fig. 2A). Cells were immortalized by retroviral transduction of the SV40 large T antigen (Jat and Sharp, 1986).

Establishment of MEF cell lines lacking functional Abi1/Hssh3bp1 gene following Cre-mediated deletion of exon 1. Clone #3 and clone #8 were used for production of Abi1/Hssh3bp1 deletion lines. Disruption of the Abi1/Hssh3bp1 gene by deletion of exon 1 was achieved by transient transfection with Cre-recombinase using a plasmid conferring resistance to puromycin (Taniguchi et al., 1998). Genomic deletion of Abi1/Hssh3bp1 exon 1 was confirmed by genotyping with several PCR primer sets (see Materials and Methods), including primers DL75' and Neogene 13' (Fig. 2B), and by sequencing PCR products. Western blot analysis (Fig. 2C) demonstrated the lack of Abi1/Hssh3bp1 protein expression in the clones. Representative data from 11 subclones of the parental MEF clone #3 are presented in (Fig. 2C).

Analysis of cell morphology of cells lacking Abi1/Hssh3bp1 gene expression.

Abi1/Hssh3bp1 is localized to PDGF-stimulated peripheral and dorsal ruffles in precursor (fl/fl) cells, but is absent from knockout MEF cells. Abi1/Hssh3bp1 is known to be involved in actin reorganization resulting in lamellipodia, and in actin-rich peripheral and dorsal ruffle formation. Therefore we asked whether Abi1/Hssh3bp1 localizes to these structures in isolated MEF cells and whether any defect in these structures is observed in cells lacking expression of a functional Abi1/Hssh3bp1 gene.

Upon PDGF treatment, both Abi1/Hssh3bp1 (fl/fl) control (# 3) and Abi1/Hssh3bp1 deficient (# 3-11) cells display peripheral as well as dorsal ruffle formation, although dorsal ruffling is less prominent in the Abi1/Hssh3bp1 KO cell line. Abi1 is highly enriched in dorsal ruffles and localizes at the tip of ruffles in the cell periphery in Abi1/Hssh3bp1 control cells, while it cannot be detected in the Abi1/Hssh3bp1 knockout cell line. Abi2 is also present in both cell lines, but in the Abi1/Hssh3bp1 control cells, it cannot be distinguished from Abi1/Hssh3bp1 localization (Fig. 3A). Thus, we have confirmed the participation of Abi1/Hssh3bp1 in the formation of circular and peripheral ruffles in control (fl/fl) MEF cells and the absence of Abi1/Hssh3bp1 in knockout MEF cells.

Quantification of peripheral and dorsal ruffle formation in Abi1/Hssh3bp1 knockout MEF cells. PDGF stimulation of Abi1/Hssh3bp1 MEF cell lines led to the formation of both peripheral and dorsal ruffling in Abi1/Hssh3bp1 control and Abi1/Hssh3bp1-deficient cells. Multiple cell morphologies were observed, and were quantified and classified according to the following categories: with ruffles, without ruffles, or with ambiguous cell morphology (Fig. 3B). Remarkably, lack of Abi1/Hssh3bp1 did not affect peripheral ruffle formation in a quantifyable manner, whereas dorsal ruffling was significantly reduced in all tested Abi1/Hssh3bp1 KO cell lines as compared to their respective parental controls. Abi1/Hssh3bp1 KO clone # 3-11 showed the most severe phenotype in response to PDGF treatment. Notably, the Abi1/Hssh3bp1 # 3 control cell line was stimulated to a greater extend by PDGF as compared to the Abi1/Hssh3bp1 # 8 control cell line (Fig. 3B).

No change in Rac activity was observed in cells lacking a functional Abi1/Hssh3bp1 gene. We examined Rac activity in Abi1/Hssh3bp1 MEF cell lines following PDGF treatment. The PDGF treatment caused strong Rac activation in both Abi1/Hssh3bp1 control and Abi1/Hssh3bp1-deficient cell lines (Fig. 3C). However, no significant effects were observed in the Abi1/Hssh3bp1 knockout cells. This observation suggested that Abi1/Hssh3bp1 acts either downstream of Rac or that Abi1/Hssh3bp1 function is compensated for by another protein, for instance Abi2.

Cells lacking Abi1/Hssh3bp1 exhibit cell motility defects. Abi1/Hssh3bp1 has been implicated as a regulator of actin cytoskeleton-dependent cell motility as part of the Wave 2 complex. Therefore, we examined Abi1/Hssh3bp1 KO MEF cell lines in a series of motility assays (Fig. 4). These assays indicated reduced random cell motility (migration rate and migration distance), but increased directional persistence of cells lacking Abi1/Hssh3bp1. In the wound-healing assay, experiments indicated subtle but statistically significant impairment of wound closure of cells lacking Abi1/Hssh3bp1 (Fig. 4).

Instability of the Wave complex I Abi1 KO MEF. Cell motility assays indicated defects in cell motility in Abi1/Hssh3bp1 KO cells and suggested downregulation of Wave 2 dependent actin polymerization. It is assumed that Abi1/Hssh3bp1 is a vital part of the Wave 2-Arp 2/3 activating complex, which is regulated by Rac1 activation. Interaction between Rac1 and Wave complex and Abi1 is mediated by Nap1 and Sra-1. Data from RNA silencing experiments indicated that upon downregulation of individual subunits, all major components of the Wave 2 complex are coordinately down regulated (Innocenti et al., 2005; Kunda et al., 2003; Rogers et al., 2003; Steffen et al., 2006). We have investigated how gene disruption-mediated (i.e. genetic) knockout of Abi1/Hssh3bp1 affects the stability of the WAVE2 complex components. Western blot analysis demonstrated that Wave 2, Sra-1 and Nap1 expression levels were lower in Abi1 (-/-) null cells but were not completely abrogated (Fig. 5).

Breeding of Abi1/Hssh3bp1 floxed mice for prostate tissue specific knockout.

Mice homozygous for the recombinant floxed Abi1/Hssh3bp1 allele were bred with a probasin promoter driven Cre recombinase (Pb-Cre) expressing strain: B6.D2-Tg(Pbsn-Cre)4Prb (National Cancer Institute-Frederick; the Mouse Repository of the Mouse Models of Human Cancers Consortium). In these transgenic mice, the prostate-specific promoter of the rat probasin gene (Pb) regulates expression of Cre recombinase, hence the enzyme is expected to be expressed only in mature prostate-tissue (Wu et al., 2001). The Pb-Cre strain is maintained in the hemizygous state by breeding to C57BL/6Jfemales. Cre must be transmitted through the male mice to avoid small, but significant oocyte-mediated recombination. Breeding pairs were supplied as a hemizygous male and a female C57BL/6N mate. Successive generations of Pb-Cre mice were bred to C57BL/6J mice to generate sufficient Pb-Cre mice for experiments. Mice were genotyped using tail-obtained DNA.

Prostate specific deletion of Abi1/Hssh3bp1 exon 1 was confirmed in prostate tissue by genotyping with primers DL75’ and Flankneo13’ (Fig. 6A). This result confirms the

functionality of the loxP sites in vivo, and demonstrates the suitability of these mice for studies of Abi1/Hssh3bp1 gene function.

Proliferation rates of cells lacking Abi1/Hssh3bp1 are higher than control Abi1/Hssh3bp1(fl/fl) MEF cells. Loss of Abi1/Hsshb3p1 in primary prostate tumors and subsequent identification of primary tumor mutations that lead to disruption of Abi1/Hsshb3p1 function suggested the hypothesis that loss of Abi1/Hsshb3p1 protein leads to dysregulation of cell growth. We tested this hypothesis using MEF cells isolated from the Abi1/Hssh3bp1 conditional KO mice. Consistent with the tumor suppressor hypothesis, enhanced proliferation rates as determined by activity of mitochondrial dehydrogenase were observed in MEF Abi1/Hsshb3p1 (-/-) cells (clone #3-11) in comparison to parental clone #3 Abi1 (+/+) (**Fig. 6B)**. Primers DL75' and Flankneo13' were used for genotyping.

Literature cited

Abbondanzo, S.J., I. Gadi, and C.L. Stewart. 1993. Derivation of embryonic stem cell lines. *Methods Enzymol*. 225:803-23.

Abou-Kheir, W., B. Isaac, H. Yamaguchi, and D. Cox. 2008. Membrane targeting of WAVE2 is not sufficient for WAVE2-dependent actin polymerization: a role for IRSp53 in mediating the interaction between Rac and WAVE2. *J Cell Sci*. 121:379-90.

Abraham, R.T., and J.J. Gibbons. 2007. The mammalian target of rapamycin signaling pathway: twists and turns in the road to cancer therapy. *Clin Cancer Res*. 13:3109-14.

Amyere, M., M. Mettlen, P. Van Der Smissen, A. Platek, B. Payrastre, A. Veithen, and P.J. Courtoy. 2002. Origin, originality, functions, subversions and molecular signalling of macropinocytosis. *Int J Med Microbiol*. 291:487-94.

Amyere, M., B. Payrastre, U. Krause, P. Van Der Smissen, A. Veithen, and P.J. Courtoy. 2000. Constitutive macropinocytosis in oncogene-transformed fibroblasts depends on sequential permanent activation of phosphoinositide 3-kinase and phospholipase C. *Mol Biol Cell*. 11:3453-67.

Araki, N., Y. Egami, Y. Watanabe, and T. Hatae. 2007. Phosphoinositide metabolism during membrane ruffling and macropinosome formation in EGF-stimulated A431 cells. *Exp Cell Res*. 313:1496-507.

Araki, N., M.T. Johnson, and J.A. Swanson. 1996. A role for phosphoinositide 3-kinase in the completion of macropinocytosis and phagocytosis by macrophages. *J Cell Biol*. 135:1249-60.

Aspenstrom, P. 2004. Integration of signalling pathways regulated by small GTPases and calcium. *Biochim Biophys Acta*. 1742:51-8.

Azam, M., R.R. Latek, and G.Q. Daley. 2003. Mechanisms of autoinhibition and STI-571/imatinib resistance revealed by mutagenesis of BCR-ABL. *Cell*. 112:831-43.

Bar-Sagi, D., and J.R. Feramisco. 1986. Induction of membrane ruffling and fluid-phase pinocytosis in quiescent fibroblasts by ras proteins. *Science*. 233:1061-8.

Batchelor, C.L., and S.J. Winder. 2006. Sparks, signals and shock absorbers: how dystrophin loss causes muscular dystrophy. *Trends Cell Biol*. 16:198-205.

Bennett, V., and A.J. Baines. 2001. Spectrin and ankyrin-based pathways: metazoan inventions for integrating cells into tissues. *Physiol Rev*. 81:1353-92.

Berfield, A.K., A. Chait, J.F. Oram, R.A. Zager, A.C. Johnson, and C.K. Abrass. 2006. IGF-1 induces rat glomerular mesangial cells to accumulate triglyceride. *Am J Physiol Renal Physiol*. 290:F138-47.

Biesova, Z., C. Piccoli, and W.T. Wong. 1997. Isolation and characterization of e3B1, an eps8 binding protein that regulates cell growth. *Oncogene*. 14:233-41.

Bogdan, S., R. Stephan, C. Lobke, A. Mertens, and C. Klambt. 2005. Abi activates WASP to promote sensory organ development. *Nat Cell Biol*. 7:977-84.

Boyle, S.N., G.A. Michaud, B. Schweitzer, P.F. Predki, and A.J. Koleske. 2007. A critical role for cortactin phosphorylation by Abl-family kinases in PDGF-induced dorsal-wave formation. *Curr Biol*. 17:445-51.

Bryant, D.M., M.C. Kerr, L.A. Hammond, S.R. Joseph, K.E. Mostov, R.D. Teasdale, and J.L. Stow. 2007. EGF induces macropinocytosis and SNX1-modulated recycling of E-cadherin. *J Cell Sci*. 120:1818-28.

Cardelli, J. 2001. Phagocytosis and macropinocytosis in Dictyostelium: phosphoinositide-based processes, biochemically distinct. *Traffic*. 2:311-20.

Courtney, K.D., M. Grove, H. Vandongen, A. Vandongen, A.S. LaMantia, and A.M. Pendergast. 2000. Localization and phosphorylation of Abl-interactor proteins, Abi-1 and Abi-2, in the developing nervous system. *Mol Cell Neurosci*. 16:244-57.

Dai, Z., and A.M. Pendergast. 1995. Abi-2, a novel SH3-containing protein interacts with the c-Abl tyrosine kinase and modulates c-Abl transforming activity. *Genes Dev*. 9:2569-82.

Davies, P.F., and R. Ross. 1978. Mediation of pinocytosis in cultured arterial smooth muscle and endothelial cells by platelet-derived growth factor. *J Cell Biol*. 79:663-71.

De Matteis, M.A., and J.S. Morrow. 2000. Spectrin tethers and mesh in the biosynthetic pathway. *J Cell Sci*. 113 (Pt 13):2331-43.

Dharmawardhane, S., A. Schurmann, M.A. Sells, J. Chernoff, S.L. Schmid, and G.M. Bokoch. 2000. Regulation of macropinocytosis by p21-activated kinase-1. *Mol Biol Cell*. 11:3341-52.

Druker, B.J. 2006. Circumventing resistance to kinase-inhibitor therapy. *N Engl J Med*. 354:2594-6.

Echarri, A., M.J. Lai, M.R. Robinson, and A.M. Pendergast. 2004. Abl interactor 1 (Abi-1) wave-binding and SNARE domains regulate its nucleocytoplasmic shuttling, lamellipodium localization, and wave-1 levels. *Mol Cell Biol*. 24:4979-93.

Faix, J., and R. Grosse. 2006. Staying in shape with formins. *Dev Cell*. 10:693-706.

Falcone, S., E. Cocucci, P. Podini, T. Kirchhausen, E. Clementi, and J. Meldolesi. 2006. Macropinocytosis: regulated coordination of endocytic and exocytic membrane traffic events. *J Cell Sci*. 119:4758-69.

Fiorentini, C., L. Falzano, S. Travaglione, and A. Fabbri. 2003. Hijacking Rho GTPases by protein toxins and apoptosis: molecular strategies of pathogenic bacteria. *Cell Death Differ*. 10:147-52.

Funato, Y., T. Terabayashi, N. Suenaga, M. Seiki, T. Takenawa, and H. Miki. 2004. IRSp53/Eps8 complex is important for positive regulation of Rac and cancer cell motility/invasiveness. *Cancer Res*. 64:5237-44.

Gallagher, P.G., and R.A. Ehrenkranz. 1993. Erythropoietin therapy for anemia of prematurity. *Clin Perinatol*. 20:169-91.

Gautreau, A., H.Y. Ho, J. Li, H. Steen, S.P. Gygi, and M.W. Kirschner. 2004. Purification and architecture of the ubiquitous Wave complex. *Proc Natl Acad Sci U S A*. 101:4379-83.

Goley, E.D., T. Ohkawa, J. Mancuso, J.B. Woodruff, J.A. D'Alessio, W.Z. Cande, L.E. Volkman, and M.D. Welch. 2006. Dynamic nuclear actin assembly by Arp2/3 complex and a baculovirus WASP-like protein. *Science*. 314:464-7.

Goodman, S.R., W.E. Zimmer, M.B. Clark, I.S. Zagon, J.E. Barker, and M.L. Bloom. 1995. Brain spectrin: of mice and men. *Brain Res Bull*. 36:593-606.

Gouin, E., M.D. Welch, and P. Cossart. 2005. Actin-based motility of intracellular pathogens. *Curr Opin Microbiol*. 8:35-45.

Haigler, H.T., J.A. McKanna, and S. Cohen. 1979. Rapid stimulation of pinocytosis in human carcinoma cells A-431 by epidermal growth factor. *J Cell Biol*. 83:82-90.

Hall, A. 1998. Rho GTPases and the actin cytoskeleton. *Science*. 279:509-14.

Hewlett, L.J., A.R. Prescott, and C. Watts. 1994. The coated pit and macropinocytic pathways serve distinct endosome populations. *J Cell Biol*. 124:689-703.

Ibarra, N., A. Pollitt, and R.H. Insall. 2005. Regulation of actin assembly by SCAR/WAVE proteins. *Biochem Soc Trans*. 33:1243-6.

Ikeguchi, A., H.Y. Yang, G. Gao, and S.P. Goff. 2001. Inhibition of v-Abl transformation in 3T3 cells overexpressing different forms of the Abelson interactor protein Abi-1. *Oncogene*. 20:4926-34.

Innocenti, M., E. Frittoli, I. Ponzanelli, J.R. Falck, S.M. Brachmann, P.P. Di Fiore, and G. Scita. 2003. Phosphoinositide 3-kinase activates Rac by entering in a complex with Eps8, Abi1, and Sos-1. *J Cell Biol*. 160:17-23.

Innocenti, M., S. Gerboth, K. Rottner, F.P. Lai, M. Hertzog, T.E. Stradal, E. Frittoli, D. Didry, S. Polo, A. Disanza, S. Benesch, P.P. Di Fiore, M.F. Carlier, and G. Scita. 2005. Abi1 regulates the activity of N-WASP and WAVE in distinct actin-based processes. *Nat Cell Biol*. 7:969-76.

Innocenti, M., A. Zucconi, A. Disanza, E. Frittoli, L.B. Areces, A. Steffen, T.E. Stradal, P.P. Di Fiore, M.F. Carlier, and G. Scita. 2004. Abi1 is essential for the formation and activation of a WAVE2 signalling complex. *Nat Cell Biol*. 6:319-27.

Ittmann, M.M. 1998. Chromosome 10 alterations in prostate adenocarcinoma (review). *Oncol Rep*. 5:1329-35.

Jat, P.S., and P.A. Sharp. 1986. Large T antigens of simian virus 40 and polyomavirus efficiently establish primary fibroblasts. *J Virol*. 59:746-50.

Jin, H., and J.Y. Wang. 2007. Abl tyrosine kinase promotes dorsal ruffles but restrains lamellipodia extension during cell spreading on fibronectin. *Mol Biol Cell*. 18:4143-54.

Joiner, C.H., R.S. Franco, M. Jiang, M.S. Franco, J.E. Barker, and S.E. Lux. 1995. Increased cation permeability in mutant mouse red blood cells with defective membrane skeletons. *Blood*. 86:4307-14.

Jones, M.C., P.T. Caswell, and J.C. Norman. 2006. Endocytic recycling pathways: emerging regulators of cell migration. *Curr Opin Cell Biol*. 18:549-57.

Jung, J.H., A.M. Pendergast, P.A. Zipfel, and J.A. Traugh. 2008. Phosphorylation of c-Abl by protein kinase Pak2 regulates differential binding of ABI2 and CRK. *Biochemistry*. 47:1094-104.

Kharas, M.G., and D.A. Fruman. 2005. ABL oncogenes and phosphoinositide 3-kinase: mechanism of activation and downstream effectors. *Cancer Res*. 65:2047-53.

Kotula, L., T.M. DeSilva, D.W. Speicher, and P.J. Curtis. 1993. Functional characterization of recombinant human red cell alpha-spectrin polypeptides containing the tetramer binding site. *J Biol Chem*. 268:14788-93.

Kotula, L., L.D. Laury-Kleintop, L. Showe, K. Sahr, A.J. Linnenbach, B. Forget, and P.J. Curtis. 1991. The exon-intron organization of the human erythrocyte alpha-spectrin gene. *Genomics*. 9:131-40.

Kovar, D.R., and T.D. Pollard. 2004. Insertional assembly of actin filament barbed ends in association with formins produces piconewton forces. *Proc Natl Acad Sci U S A*. 101:14725-30.

Krysko, D.V., G. Denecker, N. Festjens, S. Gabriels, E. Parthoens, K. D'Herde, and P. Vandenabeele. 2006. Macrophages use different internalization mechanisms to clear apoptotic and necrotic cells. *Cell Death Differ*. 13:2011-22.

Kunda, P., G. Craig, V. Dominguez, and B. Baum. 2003. Abi, Sra1, and Kette control the stability and localization of SCAR/WAVE to regulate the formation of actin-based protrusions. *Curr Biol*. 13:1867-75.

Leng, Y., J. Zhang, K. Badour, E. Arpaia, S. Freeman, P. Cheung, M. Siu, and K. Siminovitch. 2005. Abelson-interactor-1 promotes WAVE2 membrane translocation and Abelson-mediated tyrosine phosphorylation required for WAVE2 activation. *Proc Natl Acad Sci U S A*. 102:1098-103.

Liberali, P., E. Kakkonen, G. Turacchio, C. Valente, A. Spaar, G. Perinetti, R.A. Bockmann, D. Corda, A. Colanzi, V. Marjomaki, and A. Luini. 2008. The closure of Pak1-dependent macropinosomes requires the phosphorylation of CtBP1/BARS. *Embo J*. 27:970-81.

Macoska, J.A., J. Xu, D. Ziemnicka, T.S. Schwab, M.A. Rubin, and L. Kotula. 2001. Loss of expression of human spectrin src homology domain binding protein 1 is associated with 10p loss in human prostatic adenocarcinoma. *Neoplasia*. 3:99-104.

Meier, O., and U.F. Greber. 2004. Adenovirus endocytosis. *J Gene Med*. 6 Suppl 1:S152-63.

Mischel, P.S., and T. Cloughesy. 2006. Using molecular information to guide brain tumor therapy. *Nat Clin Pract Neurol*. 2:232-3.

Miyata, Y., M. Hoshi, S. Koyasu, T. Kadowaki, M. Kasuga, I. Yahara, E. Nishida, and H. Sakai. 1988. Rapid stimulation of fluid-phase endocytosis and exocytosis by insulin, insulin-like growth factor-I, and epidermal growth factor in KB cells. *Exp Cell Res*. 178:73-83.

Nagy, A.G., Marina; Vintersten, Kristina; Behringer, Richard. 2003. Manipulating the mouse embryo: a laboratory manual. Cold Spring Harbor Laboratory Press Cold Spring Harbor. 764 pp.

Narla, G., S.L. Friedman, and J.A. Martignetti. 2003. Kruppel cripples prostate cancer: KLF6 progress and prospects. *Am J Pathol*. 162:1047-52.

Nichols, B.J., and J. Lippincott-Schwartz. 2001. Endocytosis without clathrin coats. *Trends Cell Biol*. 11:406-12.

Niedergang, F., and P. Chavrier. 2005. Regulation of phagocytosis by Rho GTPases. *Curr Top Microbiol Immunol*. 291:43-60.

Norbury, C.C. 2006. Drinking a lot is good for dendritic cells. *Immunology*. 117:443-51.

Offenhauser, N., A. Borgonovo, A. Disanza, P. Romano, I. Ponzanelli, G. Iannolo, P.P. Di Fiore, and G. Scita. 2004. The eps8 family of proteins links growth factor stimulation to actin reorganization generating functional redundancy in the Ras/Rac pathway. *Mol Biol Cell*. 15:91-8.

Oikawa, T., H. Yamaguchi, T. Itoh, M. Kato, T. Ijuin, D. Yamazaki, S. Suetsugu, and T. Takenawa. 2004. PtdIns(3,4,5)P3 binding is necessary for WAVE2-induced formation of lamellipodia. *Nat Cell Biol*. 6:420-6.

Patel, J.C., and J.E. Galan. 2005. Manipulation of the host actin cytoskeleton by Salmonella--all in the name of entry. *Curr Opin Microbiol*. 8:10-5.
Pollard, T.D., and G.G. Borisy. 2003. Cellular motility driven by assembly and disassembly of actin filaments. *Cell*. 112:453-65.
Pollitt, A.Y., and R.H. Insall. 2008. Abi mutants in Dictyostelium reveal specific roles for the SCAR/WAVE complex in cytokinesis. *Curr Biol*. 18:203-10.
Porat-Shliom, N., Y. Kloog, and J.G. Donaldson. 2008. A Unique Platform for H-Ras Signaling Involving Clathrin-independent Endocytosis. *Mol Biol Cell*. 19:765-75.
Racoosin, E.L., and J.A. Swanson. 1992. M-CSF-induced macropinocytosis increases solute endocytosis but not receptor-mediated endocytosis in mouse macrophages. *J Cell Sci*. 102 (Pt 4):867-80.
Ridley, A.J. 2006. Rho GTPases and actin dynamics in membrane protrusions and vesicle trafficking. *Trends Cell Biol.* 16:522-9.
Ridley, A.J., H.F. Paterson, C.L. Johnston, D. Diekmann, and A. Hall. 1992. The small GTP-binding protein rac regulates growth factor-induced membrane ruffling. *Cell*. 70:401-10.
Rogers, S.L., U. Wiedemann, N. Stuurman, and R.D. Vale. 2003. Molecular requirements for actin-based lamella formation in Drosophila S2 cells. *J Cell Biol.* 162:1079-88.
Rottner, K., T.E. Stradal, and J. Wehland. 2005. Bacteria-host-cell interactions at the plasma membrane: stories on actin cytoskeleton subversion. *Dev Cell*. 9:3-17.
Sadowski, P.D. 1995. The Flp recombinase of the 2-microns plasmid of Saccharomyces cerevisiae. *Prog Nucleic Acid Res Mol Biol.* 51:53-91.
Sauer, B., and N. Henderson. 1988. Site-specific DNA recombination in mammalian cells by the Cre recombinase of bacteriophage P1. *Proc Natl Acad Sci U S A*. 85:5166-70.
Scita, G., J. Nordstrom, R. Carbone, P. Tenca, G. Giardina, S. Gutkind, M. Bjarnegard, C. Betsholtz, and P.P. Di Fiore. 1999. EPS8 and E3B1 transduce signals from Ras to Rac. *Nature*. 401:290-3.
Scott, R.W., and M.F. Olson. 2007. LIM kinases: function, regulation and association with human disease. *J Mol Med.* 85:555-68.
Seastone, D.J., L. Zhang, G. Buczynski, P. Rebstein, G. Weeks, G. Spiegelman, and J. Cardelli. 1999. The small Mr Ras-like GTPase Rap1 and the phospholipase C pathway act to regulate phagocytosis in Dictyostelium discoideum. *Mol Biol Cell*. 10:393-406.
Shi, Y., K. Alin, and S.P. Goff. 1995. Abl-interactor-1, a novel SH3 protein binding to the carboxy-terminal portion of the Abl protein, suppresses v-abl transforming activity. *Genes Dev*. 9:2583-97.
Skeen, J.E., P.T. Bhaskar, C.C. Chen, W.S. Chen, X.D. Peng, V. Nogueira, A. Hahn-Windgassen, H. Kiyokawa, and N. Hay. 2006. Akt deficiency impairs normal cell proliferation and suppresses oncogenesis in a p53-independent and mTORC1-dependent manner. *Cancer Cell*. 10:269-80.
Steffen, A., J. Faix, G.P. Resch, J. Linkner, J. Wehland, J.V. Small, K. Rottner, and T.E. Stradal. 2006. Filopodia formation in the absence of functional WAVE- and Arp2/3-complexes. *Mol Biol Cell*. 17:2581-91.

Steffen, A., K. Rottner, J. Ehinger, M. Innocenti, G. Scita, J. Wehland, and T.E. Stradal. 2004. Sra-1 and Nap1 link Rac to actin assembly driving lamellipodia formation. *Embo J*. 23:749-59.

Sternberg, N., and D. Hamilton. 1981. Bacteriophage P1 site-specific recombination. I. Recombination between loxP sites. *J Mol Biol*. 150:467-86.

Stovold, C.F., T.H. Millard, and L.M. Machesky. 2005. Inclusion of Scar/WAVE3 in a similar complex to Scar/WAVE1 and 2. *BMC Cell Biol.* 6:11.

Stradal, T., K.D. Courtney, K. Rottner, P. Hahne, J.V. Small, and A.M. Pendergast. 2001. The Abl interactor proteins localize to sites of actin polymerization at the tips of lamellipodia and filopodia. *Curr Biol.* 11:891-5.

Stradal, T.E., K. Rottner, A. Disanza, S. Confalonieri, M. Innocenti, and G. Scita. 2004. Regulation of actin dynamics by WASP and WAVE family proteins. *Trends Cell Biol*. 14:303-11.

Stradal, T.E., and G. Scita. 2006. Protein complexes regulating Arp2/3-mediated actin assembly. *Curr Opin Cell Biol*. 18:4-10.

Suetsugu, S., S. Kurisu, T. Oikawa, D. Yamazaki, A. Oda, and T. Takenawa. 2006. Optimization of WAVE2 complex-induced actin polymerization by membrane-bound IRSp53, PIP(3), and Rac. *J Cell Biol*. 173:571-85.

Suetsugu, S., D. Yamazaki, S. Kurisu, and T. Takenawa. 2003. Differential roles of WAVE1 and WAVE2 in dorsal and peripheral ruffle formation for fibroblast cell migration. *Dev Cell*. 5:595-609.

Swanson, J.A., and C. Watts. 1995. Macropinocytosis. *Trends Cell Biol*. 5:424-8.

Takenawa, T., and S. Suetsugu. 2007. The WASP-WAVE protein network: connecting the membrane to the cytoskeleton. *Nat Rev Mol Cell Biol.* 8:37-48.

Taniguchi, M., M. Sanbo, S. Watanabe, I. Naruse, M. Mishina, and T. Yagi. 1998. Efficient production of Cre-mediated site-directed recombinants through the utilization of the puromycin resistance gene, pac: a transient gene-integration marker for ES cells. *Nucleic Acids Res*. 26:679-80.

Varticovski, L., G.Q. Daley, P. Jackson, D. Baltimore, and L.C. Cantley. 1991. Activation of phosphatidylinositol 3-kinase in cells expressing abl oncogene variants. *Mol Cell Biol*. 11:1107-13.

Vega, F.M., and A.J. Ridley. 2008. Rho GTPases in cancer cell biology. *FEBS Lett.* 582:2093-2101.

Veithen, A., P. Cupers, P. Baudhuin, and P.J. Courtoy. 1996. v-Src induces constitutive macropinocytosis in rat fibroblasts. *J Cell Sci*. 109 (Pt 8):2005-12.

Waes, J.G., and R.H. Finnell. 2001. Importance of model organisms in understanding the biology and genetic basis of human nonsyndromic neural tube defects. *Teratology*. 64:177-80.

Wang, C., R. Navab, V. Iakovlev, Y. Leng, J. Zhang, M.S. Tsao, K. Siminovitch, D.R. McCready, and S.J. Done. 2007. Abelson interactor protein-1 positively regulates breast cancer cell proliferation, migration, and invasion. *Mol Cancer Res*. 5:1031-9.

Watts, C., M.A. West, P.A. Reid, and H.W. Davidson. 1989. Processing of immunoglobulin-associated antigen in B lymphocytes. *Cold Spring Harb Symp Quant Biol.* 54 Pt 1:345-52.

Welch, M.D., and R.D. Mullins. 2002. Cellular control of actin nucleation. *Annu Rev Cell Dev Biol*. 18:247-88.

West, M.A., M.S. Bretscher, and C. Watts. 1989. Distinct endocytotic pathways in epidermal growth factor-stimulated human carcinoma A431 cells. *J Cell Biol*. 109:2731-9.

West, M.A., A.R. Prescott, E.L. Eskelinen, A.J. Ridley, and C. Watts. 2000. Rac is required for constitutive macropinocytosis by dendritic cells but does not control its downregulation. *Curr Biol*. 10:839-48.

Wu, X., J. Wu, J. Huang, W.C. Powell, J. Zhang, R.J. Matusik, F.O. Sangiorgi, R.E. Maxson, H.M. Sucov, and P. Roy-Burman. 2001. Generation of a prostate epithelial cell-specific Cre transgenic mouse model for tissue-specific gene ablation. *Mech Dev*. 101:61-9.

Xiong, X., P. Cui, S. Hossain, R. Xu, B. Warner, X. Guo, X. An, A.K. Debnath, D. Cowburn, and L. Kotula. 2008. Allosteric inhibition of the nonMyristoylated c-Abl tyrosine kinase by phosphopeptides derived from Abi1/Hssh3bp1. *Biochim Biophys Acta*. 1783:737-47.

Xu, J., D. Ziemnicka, G.S. Merz, and L. Kotula. 2000. Human spectrin Src homology 3 domain binding protein 1 regulates macropinocytosis in NIH 3T3 cells. *J Cell Sci*. 113 Pt 21:3805-14.

Yamazaki, D., S. Suetsugu, H. Miki, Y. Kataoka, S. Nishikawa, T. Fujiwara, N. Yoshida, and T. Takenawa. 2003. WAVE2 is required for directed cell migration and cardiovascular development. *Nature*. 424:452-6.

Yan, C., N. Martinez-Quiles, S. Eden, T. Shibata, F. Takeshima, R. Shinkura, Y. Fujiwara, R. Bronson, S.B. Snapper, M.W. Kirschner, R. Geha, F.S. Rosen, and F.W. Alt. 2003. WAVE2 deficiency reveals distinct roles in embryogenesis and Rac-mediated actin-based motility. *Embo J*. 22:3602-12.

Yoshida, B.A., M.A. Chekmareva, J.F. Wharam, M. Kadkhodaian, W.M. Stadler, A. Boyer, K. Watabe, J.B. Nelson, and C.W. Rinker-Schaeffer. 1998. Prostate cancer metastasis-suppressor genes: a current perspective. *In Vivo*. 12:49-58.

Yu, W., X. Sun, N. Clough, E. Cobos, Y. Tao, and Z. Dai. 2008. Abi1 Gene Silencing by Short Hairpin RNA Impairs Bcr-Abl-Induced Cell Adhesion and Migration in vitro and Leukemogenesis in vivo. *Carcinogenesis*.

Zhao, B., Y. Li, C. Buono, S.W. Waldo, N.L. Jones, M. Mori, and H.S. Kruth. 2006. Constitutive receptor-independent low density lipoprotein uptake and cholesterol accumulation by macrophages differentiated from human monocytes with macrophage-colony-stimulating factor (M-CSF). *J Biol Chem*. 281:15757-62.

Ziemnicka-Kotula, D., J. Xu, H. Gu, A. Potempska, K.S. Kim, E.C. Jenkins, E. Trenkner, and L. Kotula. 1998. Identification of a candidate human spectrin Src homology 3 domain-binding protein suggests a general mechanism of association of tyrosine kinases with the spectrin-based membrane skeleton. *J Biol Chem*. 273:13681-92.

Zigmond, S.H. 2004. Beginning and ending an actin filament: control at the barbed end. *Curr Top Dev Biol*. 63:145-88.

Figure Legends

Figure 1. Production of conditional Abi1/Hssh3bp1 KO mouse. A. Design of the targeting vector. An approximately 11.8kb region used to construct the targeting vector was first subcloned from a positively identified BAC clone using a homologous recombination-based technique. The region was designed such that the short homology arm (SA) extends 1.9kb 3' to exon 1. The long homology arm (LA) ends on the 5' side of exon 1 and is approximately 9kb long. The single loxP site is inserted 5' to exon 1, and the loxP-flanked neomycin gene cassette is inserted 3' to exon 1. The neomycin gene cassette is bound by two frt sites, with one loxP site 3' to the 5' frt site. The target region is 0.9kb and includes exon 1. Locations of primers used for confirmation of the locations of loxP sites and for subsequent genotyping are indicated.

The indicated primers are as follows: a, mAbi1loxP35'; b, DL75'; c, mAbi1Intr15'; d, LAN1; e, Neogene13'; f, Flankneo13'; g, A2; h, WT1; and i, SG1. The "h" and "i" primer set (red arrows) is specific for the wild type Abi1/Hssh3bp1 gene sequence only. Primer sequences are listed in Materials and Methods (see also Fig. 1C).

B. Breeding of F1 Abi1/Hssh3bp1 heterozygous strain to remove the neomycin gene from the recombinant allele. Male and female Abi1/Hssh3bp1 heterozygous mice carrying the neomycin gene cassette was bred with the frt deletor strain 129S4/SvJaeSorGt(ROSA)26Sortm1(FLP1)Dym/J. Animals were genotyped with primers LAN1 and A2 (Materials and Methods) for the neomycin gene cassette ($Neo^+/frt^+/loxP^+$), with primers mAbi1loxP35' and Flankneo13' (Materials and Methods, and **Fig. 1C**) for the wild type allele (Wt) (upper panel, lower band) or the floxed Abi1/Hssh3bp1 allele, which is lacking the neomycin gene and the 3' frt site ($Neo^-/frt^-/loxP^+$) (upper panel, upper band). Under the PCR conditions used, no amplification of the neomycin positive allele ($Neo^+/frt^+/loxP^+$) was observed with primers mAbi1loxP35' and Flankneo13'. "Animal 1" and "Animal 3" are positive for the floxed allele lacking neomycin (these are heterozygous animals, as they each contain one copy of the wild type allele, upper panel); and they lack the neomycin gene (lower panel); "Animal 2"

contains only wild type alleles (this is a homozygous animal, as it is negative for the presence of neomycin, lower panel).

C. Abi1/Hssh3bp1 floxed allele. The coding strand sequence around the targeted exon 1 following removal of the neomycin gene elements is shown with the indicated critical elements: 5' and 3' loxP sites (highlighted in pink), exon 1 (highlighted in yellow) with the start codon **ATG** (indicated in red font), and genotyping primers. Forward sequencing primers **are bold/underlined**; reverse sequencing primers are ***bold/underlined/italics***. Sequence in small caps indicates the leftover sequence from the neomycin cassette. Within the deleted neomycin cassette the internal loxP site was also deleted (not shown here). The neomycin gene was removed by flipase-mediated recombination by breeding with frt deletor strain (**Fig. 1B**).

Figure 2. Isolation and cloning of mouse embryonic fibroblasts (MEF) lacking functional Abi1/Hssh3bp1 gene.

A. PCR-based genotyping to identify MEF cells homozygous for the recombinant Abi1 floxed allele. Left Panel, Genotyping controls for MEF cell screening. Genomic DNA obtained from the frt deletor strain and expressing only wild type alleles (lower band), and heterozygous Abi1/Hssh3bp1 (fl/+) animals expressing wild type (lower band) and Abi1/Hssh3bp1 floxed alleles (upper band), were subjected to PCR genotyping. **Right panel, Screening of MEF cells.** MEF cell DNA samples (#1-34) were isolated from mouse embryos that resulted from breeding of heterozygous Abi1/Hssh3bp1 (fl/+) animals. **Upper band,** floxed Abi1/Hssh3bp1 allele (Floxed); **Lower band,** wild type allele (Wt). Genotyping was performed using primers mAbi1loxP35' and Flankneo13'. Subsequently MEF cell lines #1, #3, #4, #6, #7, and #8 were immortalized (see Material and Methods).

B. Cre recombinase-mediated exon 1 deletion of Abi1/Hssh3bp1 gene in MEF cell lines. To obtain MEF cell lines lacking expression of the Abi1/Hssh3bp1 gene,

homozygous Abi1/Hssh3bp1 (fl/fl) cell lines #3 and #8 were transiently transfected with a puromycin-based Cre recombinase expressing plasmid. MEF cell DNA was genotyped with primers DL75' and Neogene13' (**Fig. 1C**). "Floxed", indicates Abi1/Hsshb3p1 floxed allele; "Deleted", indicates exon 1-deleted allele. Genotyping of cell lines based on the PCR result is indicated below the panel. "Abi1(fl/fl)", indicates genotype homozygous for the floxed allele; Abi1 (-/-), indicates genotype homozygous for the deleted allele; Abi1(fl/-) indicates heterozygous genotype. Note that the cell line #8-5 has both alleles indicating that in this cell line Cre recombinase failed to recombine on one allele, hence the heterozygous genotype, Abi1(fl/-), is observed. The MEF cell lines were also genotyped by another set of primers (mAbi1loxP35' and Flankneo13') confirming the observed genotypes (data not shown). Primer sequences are listed in Material and Methods; primers DL75', Neogene13' and Flankneo13' are also indicated in **Fig. 1C**.

C. Cre recombinase-mediated loss of Abi1/Hssh3bp1 protein expression in MEF#3 cell line subclones. Western blot analysis of Abi1/Hssh3bp1 expression in parental MEF#3 Abi1(fl/fl) and in exon 1 deleted Abi1(-/-) MEF cell lines, lower panel. Cell lysates of the indicated cell lines were blotted with antibody 7B6 (specific for Abi1/Hssh3bp1 (Xiong et al., 2008)). Clones "#3-1 through #3-11", represent subclones of the parental MEF#3 obtained following transient Cre recombinase expression. "Abi1 (+/+) MEF Wt" represents mouse embryonic cells expressing the wild type Abi1/Hssh3bp1 gene. "Loading control" represents part of a protein-stained gel of the same samples as used for Western blotting analysis, upper panel.

Figure 3. Evaluation of cell morphologies in Abi1/Hssh3bp1 expressing and Abi1/Hssh3bp1 knockout cell lines in response to PDGF.

A. Localization of Abi1/Hssh3bp1 in control and deficient MEF cells after PDGF-stimulation. Control (# 3) and Abi1/Hssh3bp1- KO (#3-11) cell lines were grown on glass-coverslips, starved and treated with PDGF, and immunostained with antibodies and phalloidin as described in Material and Methods. Anti-Abi1/2 antibody (W8.3) or anti

Abi1 (4E2) antibody were used. Abi1/Hssh3bp1 localizes to dorsal circular and peripheral ruffles of precursor cells but is absent in KO cells.

B. Quantification of dorsal and peripheral ruffling. MEF control (fl/fl) and Abi1/Hssh3bp1 knockout cells (KO) were plated on glass coverslips and serum-starved overnight. Cells were stimulated with PDGF, fixed and stained with Alexa Fluor 594 conjugated phalloidin to detect F-actin. The percentages of cells with different cell morphologies in response to PDGF treatment were quantified in the indicated MEF cell lines.

Dorsal circular and peripheral PDGF-induced ruffles were independently evaluated. The following categories of morphologies of PDGF response were scored: with ruffles, without ruffles, or with ambiguous cell morphology. At least 100 cells were analyzed and categorized for each condition. Columns are percentage of cells with respective morphology displayed as means ± SEMs of at least three independent experiments. #3 control, indicates parental MEF#3 cell line; #3-6 KO, #3-8 KO, and #3-11 KO, indicate MEF#3 subclones lacking Abi1/Hssh3bp1 expression; #8 indicates parental MEF cell line; #8-7, #8-11, indicate MEF #8 subclones. Dorsal circular ruffling was significantly reduced (up to 5-fold) in Abi1 knockout cell lines. Peripheral ruffling was not significantly affected in Abi1 knockout cells, with only some of the analyzed clones showing impairment.

C. PDGF-induced Rac activation is not affected in Abi1/Hssh3bp1 deficient cell lines. Abi1 control (# 3) and Abi1-deficient (# 3-6; # 3-11) cell lines were seeded in 10 cm tissue culture dishes under normal conditions. On the second day after seeding cells were serum starved for 16-18 h followed by mock treatment with DMEM or by DMEM containing PDGF (10ng/mL) for five minutes at 37 °C. The assay was performed according to the G-LISA manual. The indicated parental Abi1/Hssh3bp1(fl/fl) and Abi1/Hssh3bp1 KO (-/-) cell lines were analyzed in the assay.

Figure 4. Evaluation of cell motility of mouse embryonic fibroblasts lacking Abi1/Hssh3bp1. The parameters of random cell motility, migration distance (A), rate (B), and directional persistence (C) were evaluated in Abi1/Hsshb3p1 null cell lines (clones #3-6 and #3-11) and Abi1 floxed cells (control #3,(fl/fl)) cells. Cells were seeded under the same conditions and monitored by time-lapse video capture. Individual aspects of cell motility, n=40, were evaluated using ImageJ 1.38v program. Directional persistence was determined as the ratio of total distant traveled over total length of the migration path Abi1/Hssh3bp1 KO cells (lines #3-6 and #3-11) as compared with control #3 (fl/fl) MEF cells. D-E. Wound-healing migration assay. D. Cells were seeded under identical conditions. Following formation of a confluent monolayer, a wound was obtained by scratching with a fine pipette tip. Rate of wound closure was determined by measuring the area not covered by cells per unit of time. Data represent means ± SD of four independent assays of Abi1/Hssh3bp1 KO cell lines (#3-6 and #3-11) as compared with control #3 (fl/fl) MEF cells. E. Representative micrographs from live cell observations.

Figure 5. Evaluation of Wave complex indicates decreased expression levels of Wave2, Sra-1 and Nap1 in Abi1/Hssh3bp1 KO cells. Western blot analysis of MEF cell lysates of Abi1/Hssh3bp1 KO cell lines. WAVE 2, Nap1, and Sra-1 protein levels were evaluated with specific antibodies in total cellular lysates obtained from 2 clones (#3-6 and #3-11) lacking Abi1/Hssh3bp1 expression and from the parental line MEF#3. A significant decrease in protein levels of all analyzed proteins was observed. However, levels of protein expression vary from clone to clone suggesting that Wave complex expression is unstable following Abi1 removal. Polyclonal antibodies against Wave2, Nap1, Sra-1 (Steffen et al., 2004), and Rac1 (Material and Methods) were used. Monoclonal antibody 4E2 to Abi1/Hssh3bp1 was used.

Figure 6A. Prostate-specific disruption of the Abi1/Hssh3bp1 gene. Animals (males only) resulting from breeding of the probasin promoter driven Cre recombinase expressing strain [B6.D2-Tg(Pbsn-Cre)4Prb] with the Abi1/Hssh3bp1 floxed (fl/fl) strain were genotyped for expression of the floxed Abi1/Hssh3bp1 allele and Cre recombinase

expression. Male animals positive (+ Cre) or negative (- Cre) for Cre recombinase expression were sacrificed and prostate tissue DNA samples were evaluated by PCR genotyping for the presence of exon 1. Prostate tissue (anterior prostate and posterior prostate) from animals expressing Cre recombinase demonstrated exon 1 deletion (Deleted) in contrast to animals negative for expression of Cre (Floxed). As expected, both animals #418 and #419 were homozygous for the floxed allele, i.e., Abi1(fl/fl), in tail DNA where the probasin promoter is not active. Parental MEF #8 (Abi1 (fl/fl)) and its subcloned cell lines #8-7 and #8-11 which lack a functional Abi1/Hssh3bp1 gene (-/-) were used genotyping controls.

Figure 6B. Cells were re-plated in 96 well plates at a density of $5x10^4$ cells per well. Analysis of mitochondrial dehydrogenases (Cell Proliferation Assay, Biovision) was performed under standard (10%) serum concentration. A statistically significant difference in the enzyme activities was observed between the cells lines (**$p<0.01$).

Steffen, A., Rottner, K., Ehinger, J., Innocenti, M., Scita, G., Wehland, J. and Stradal, T. E. (2004). Sra-1 and Nap1 link Rac to actin assembly driving lamellipodia formation. *Embo J* **23**, 749-59.

Xiong, X., Cui, P., Hossain, S., Xu, R., Warner, B., Guo, X., An, X., Debnath, A. K., Cowburn, D. and Kotula, L. (2008). Allosteric inhibition of the nonMyristoylated c-Abl tyrosine kinase by phosphopeptides derived from Abi1/Hssh3bp1. *Biochim Biophys Acta* **1783**, 737-47.

Figure 1A

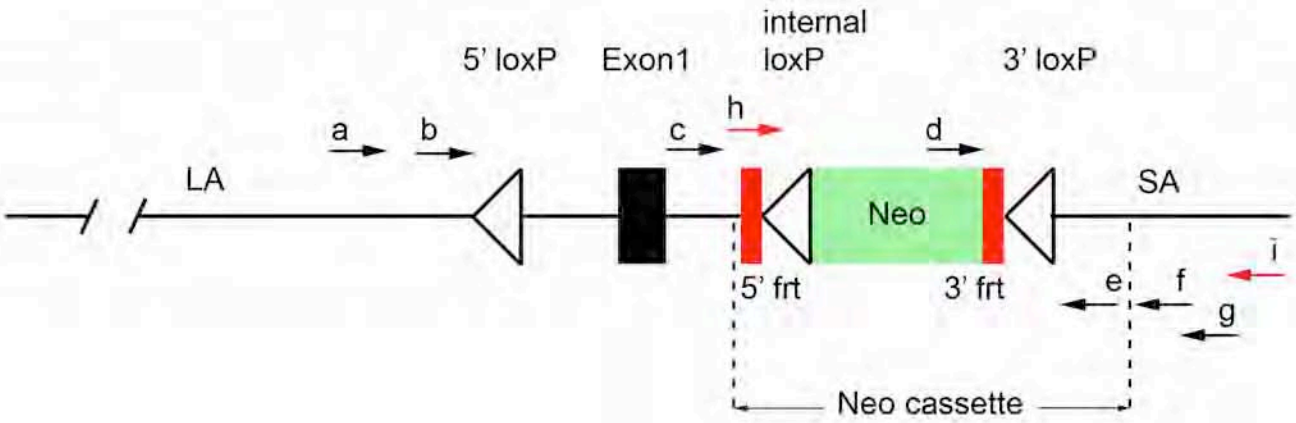
internal
5' loxP
Exon1
loxP
3' loxP
h
a
b
c
d
LA
Neo
SA
i
5' frt
3' frt
e
f
g
Neo cassette

Figure 1B

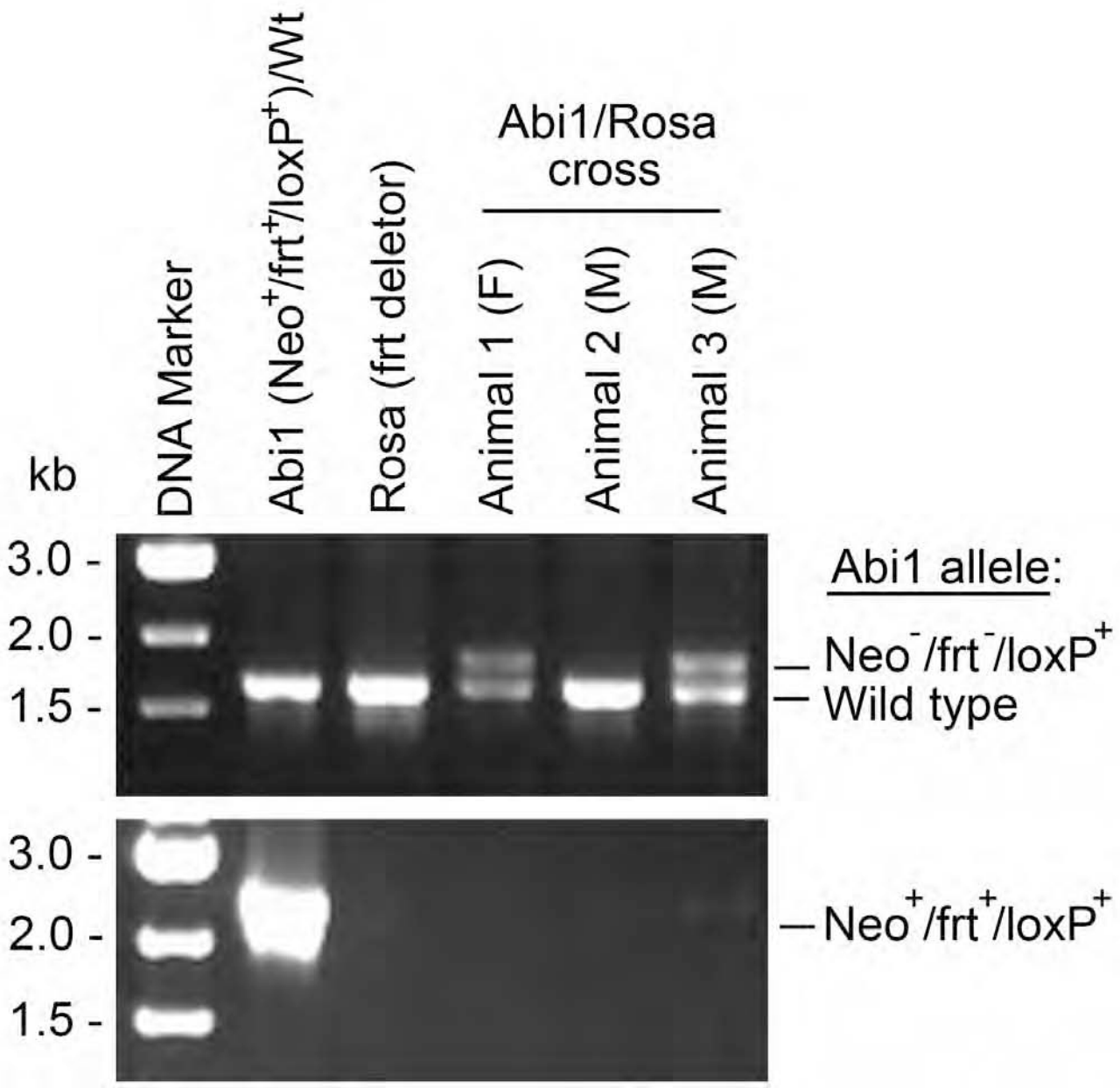
kb
DNA Marker
Abi1 (Neo+/frt+/loxP+)/Wt
Rosa (frt deletor)
Abi1/Rosa cross
Animal 1 (F)
Animal 2 (M)
Animal 3 (M)
3.0 -
2.0 -
1.5 -
Abi1 allele:
Neo-/frt-/loxP+
Wild type
3.0 -
2.0 -
1.5 -
Neo+/frt+/loxP+

Figure 1C

Abi1 floxed allele sequence

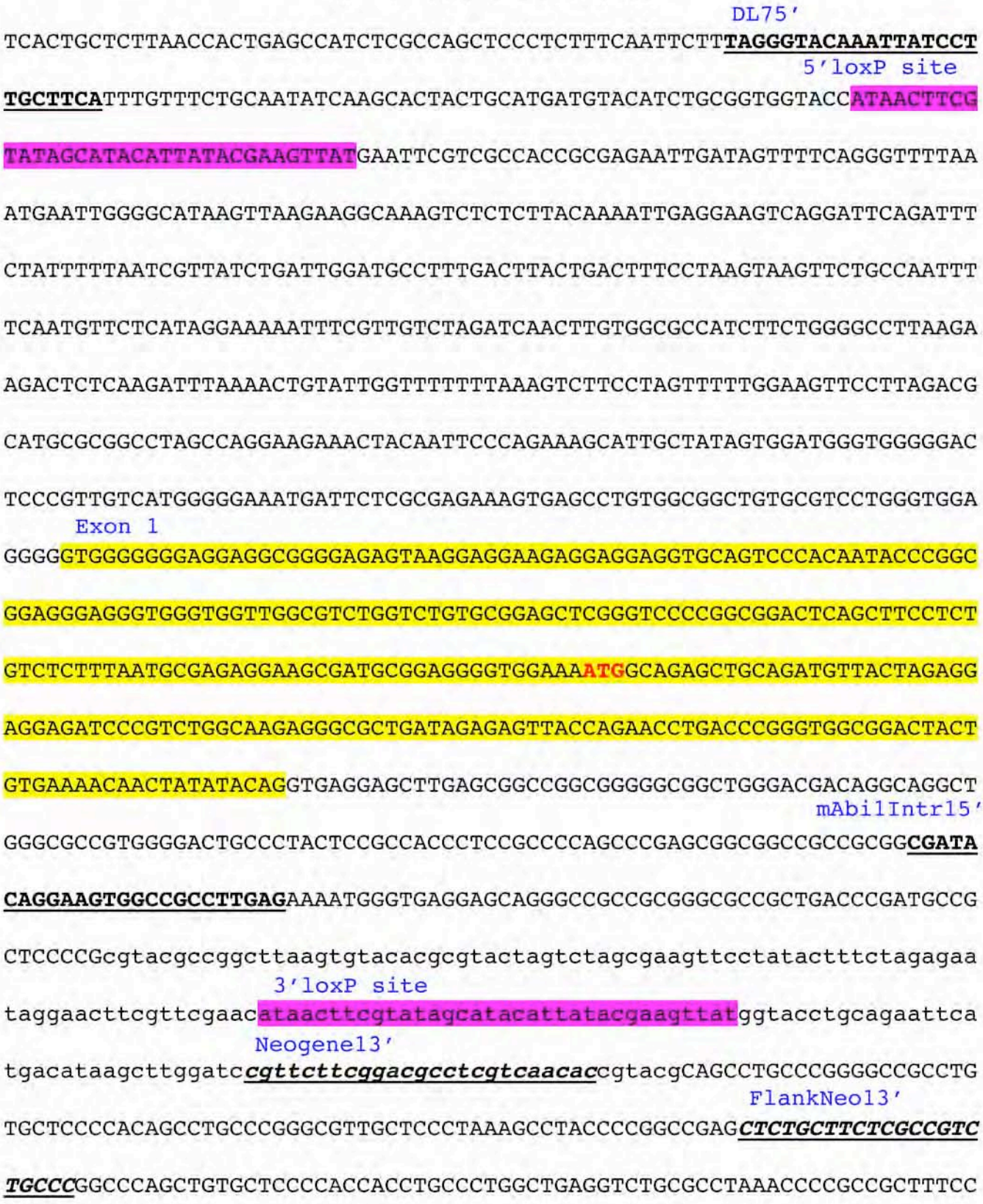

Figure 2A

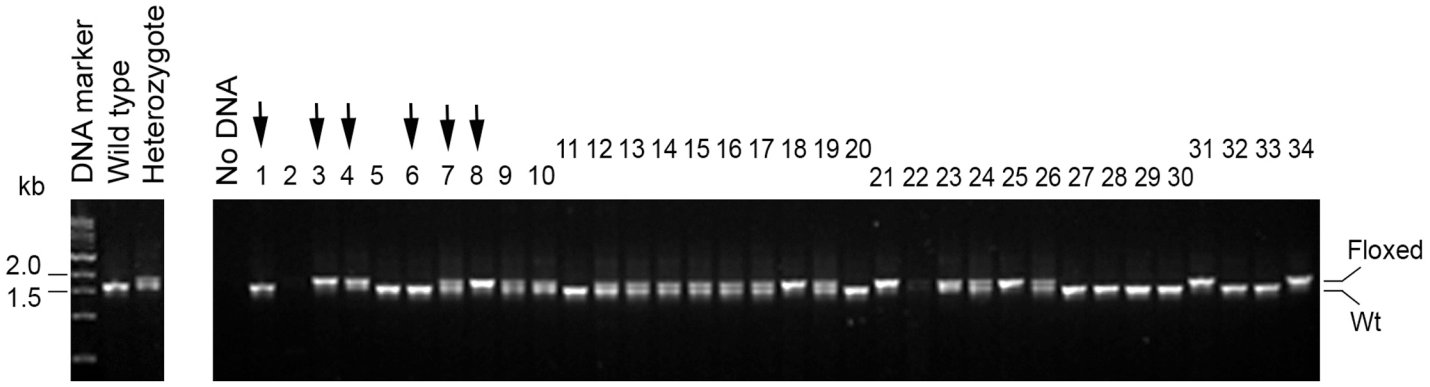
DNA marker
Wild type
Heterozygote
No DNA
kb
2.0
1.5
1 2 3 4 5 6 7 8 9 10 11 12 13 14 15 16 17 18 19 20 21 22 23 24 25 26 27 28 29 30 31 32 33 34
Floxed
Wt

Figure 2B

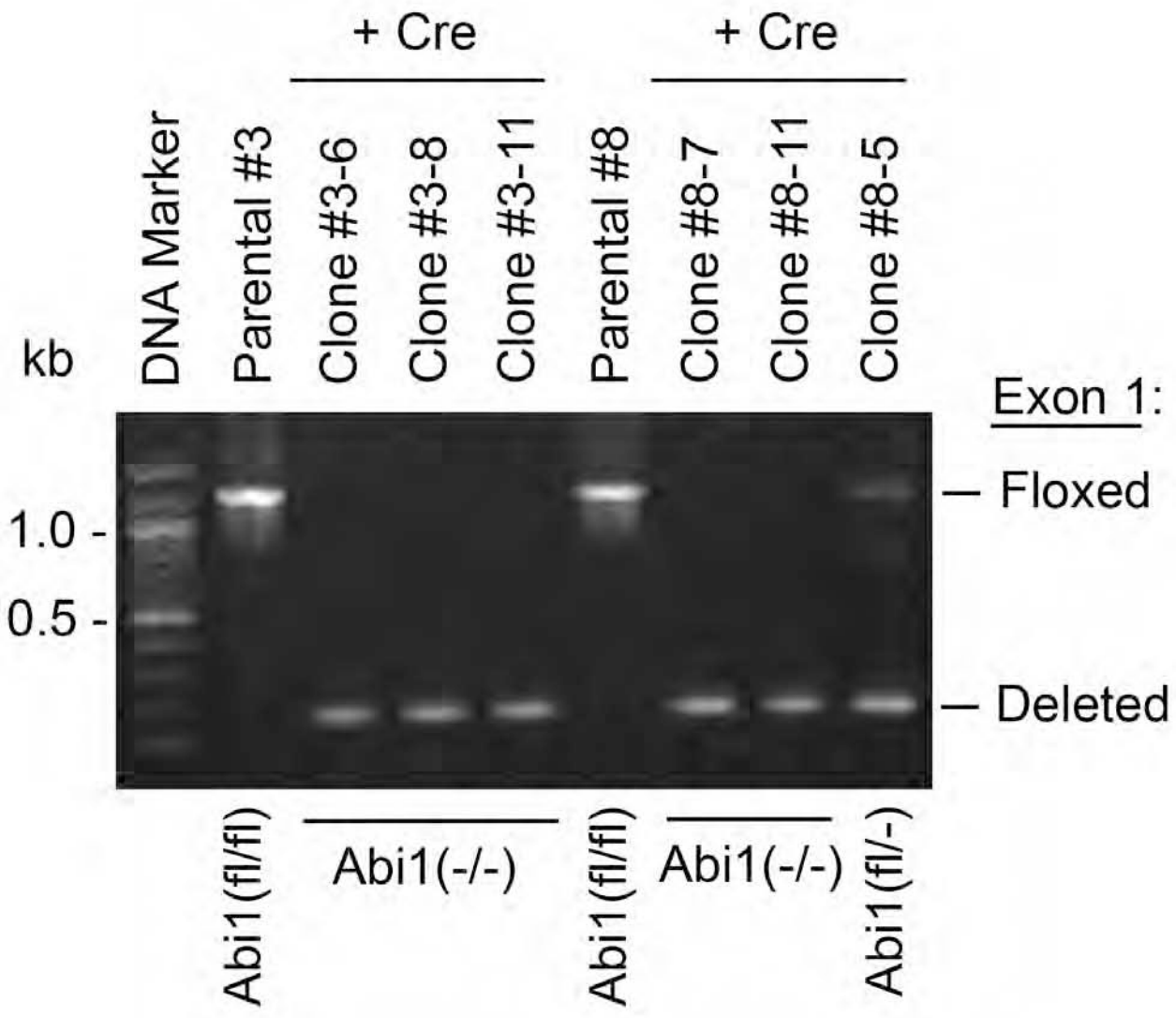
+ Cre
+ Cre
kb
DNA Marker
Parental #3
Clone #3-6
Clone #3-8
Clone #3-11
Parental #8
Clone #8-7
Clone #8-11
Clone #8-5
Exon 1:
1.0 -
0.5 -
— Floxed
— Deleted
Abi1(fl/fl)
Abi1(-/-)
Abi1(fl/fl)
Abi1(-/-)
Abi1(fl/-)

Figure 2C

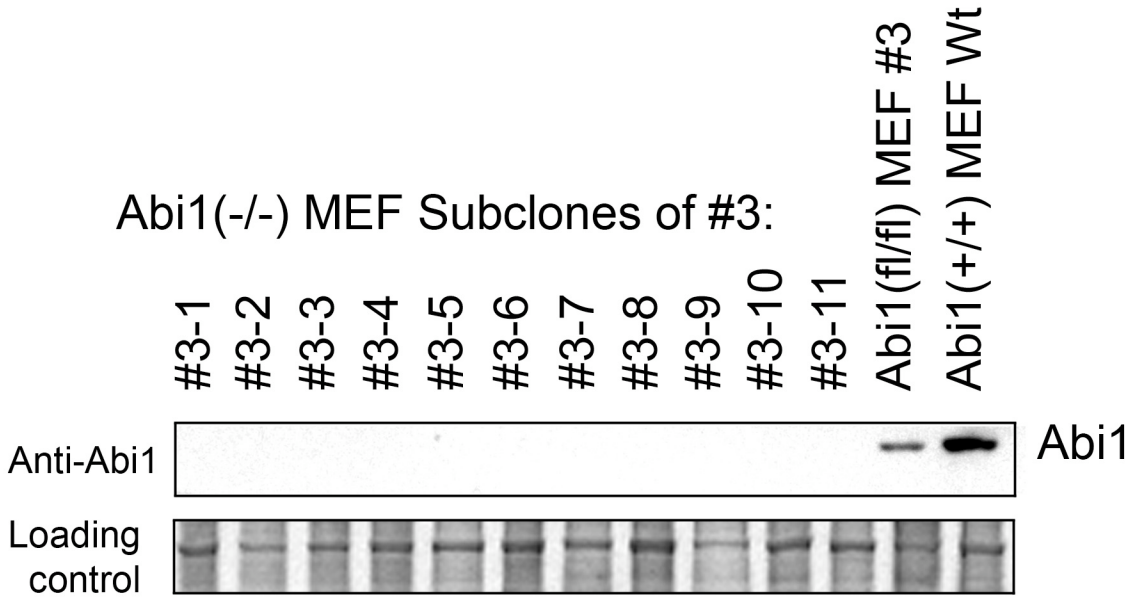
Abi1(-/-) MEF Subclones of #3:
#3-1
#3-2
#3-3
#3-4
#3-5
#3-6
#3-7
#3-8
#3-9
#3-10
#3-11
Abi1(fl/fl) MEF #3
Abi1(+/+) MEF Wt
Anti-Abi1
Abi1
Loading control

Figure 3A

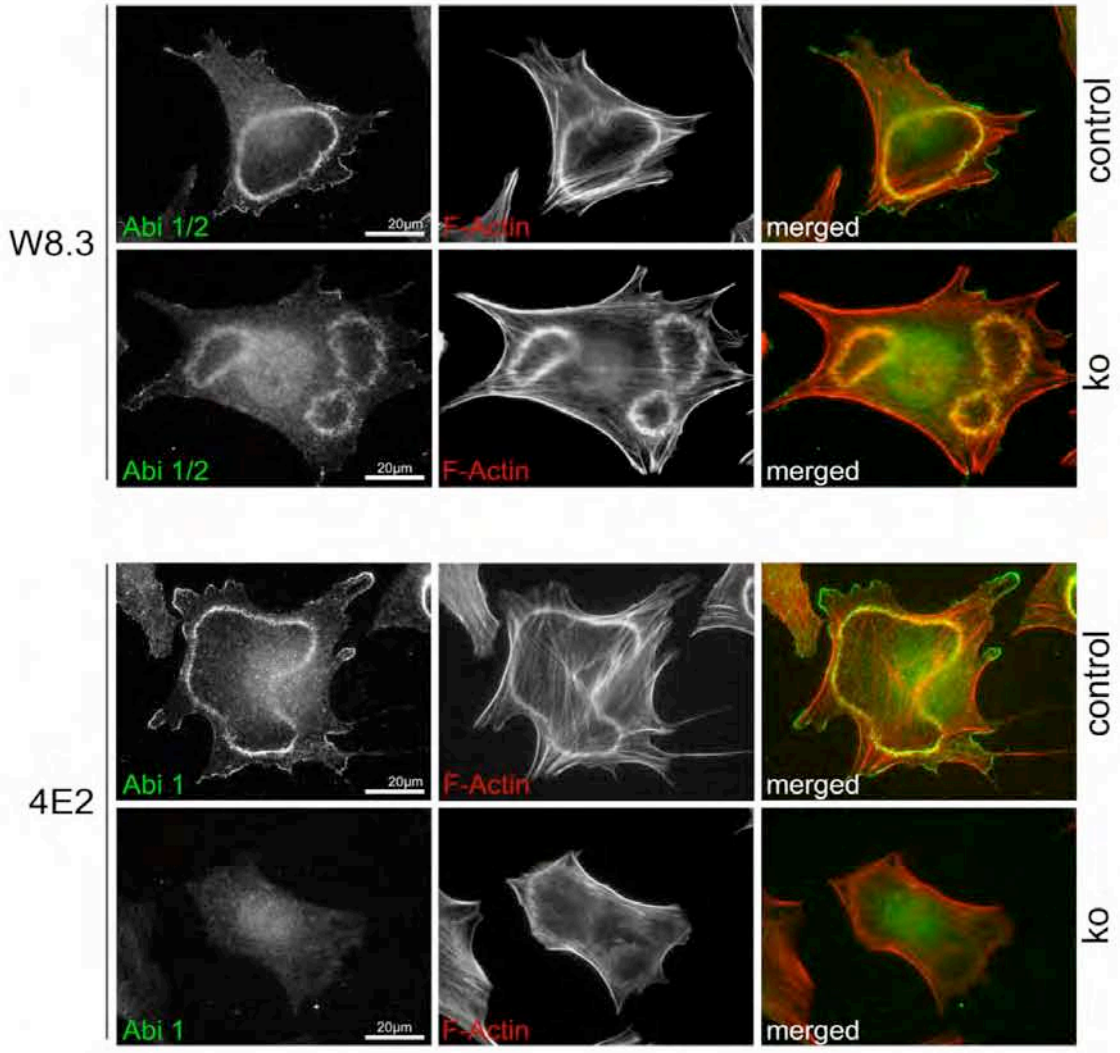
W8.3
Abi 1/2
20µm
F-Actin
merged
control
Abi 1/2
20µm
F-Actin
merged
ko
4E2
Abi 1
20µm
F-Actin
merged
control
Abi 1
20µm
F-Actin
merged
ko

Figure 3B

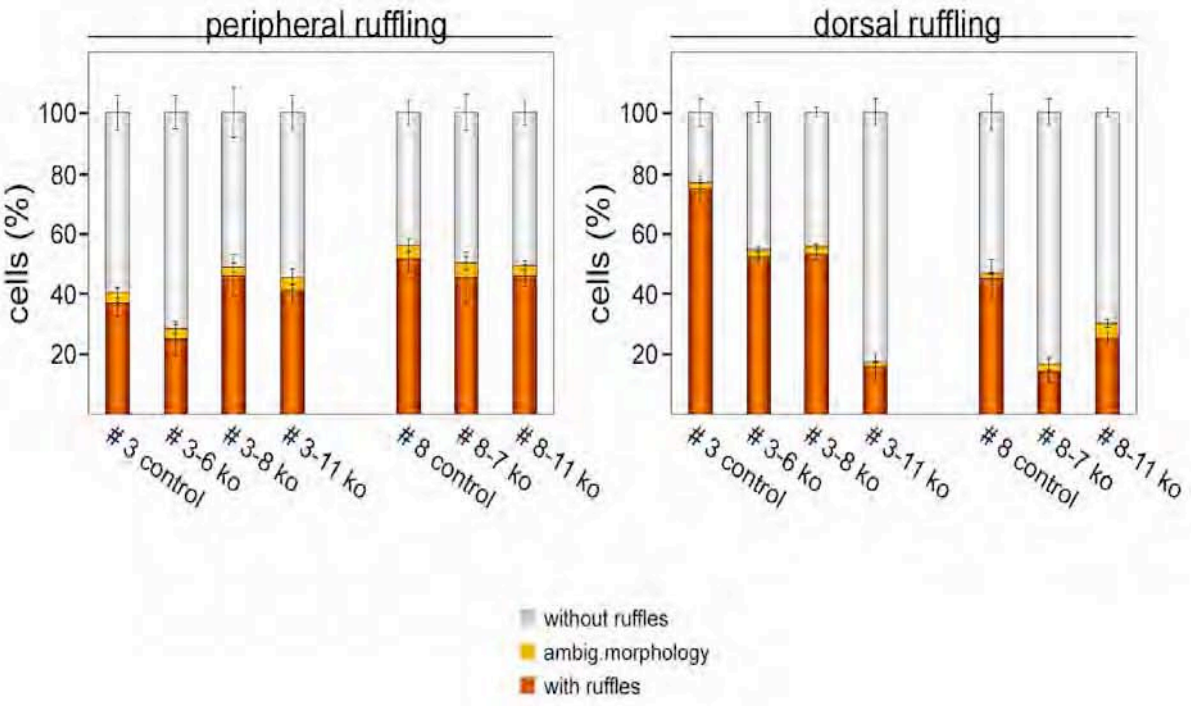
peripheral ruffling
dorsal ruffling
cells (%)
100
80
60
40
20
#3 control
#3-6 ko
#3-8 ko
#3-11 ko
#8 control
#8-7 ko
#8-11 ko
without ruffles
ambig.morphology
with ruffles

Figure 3C

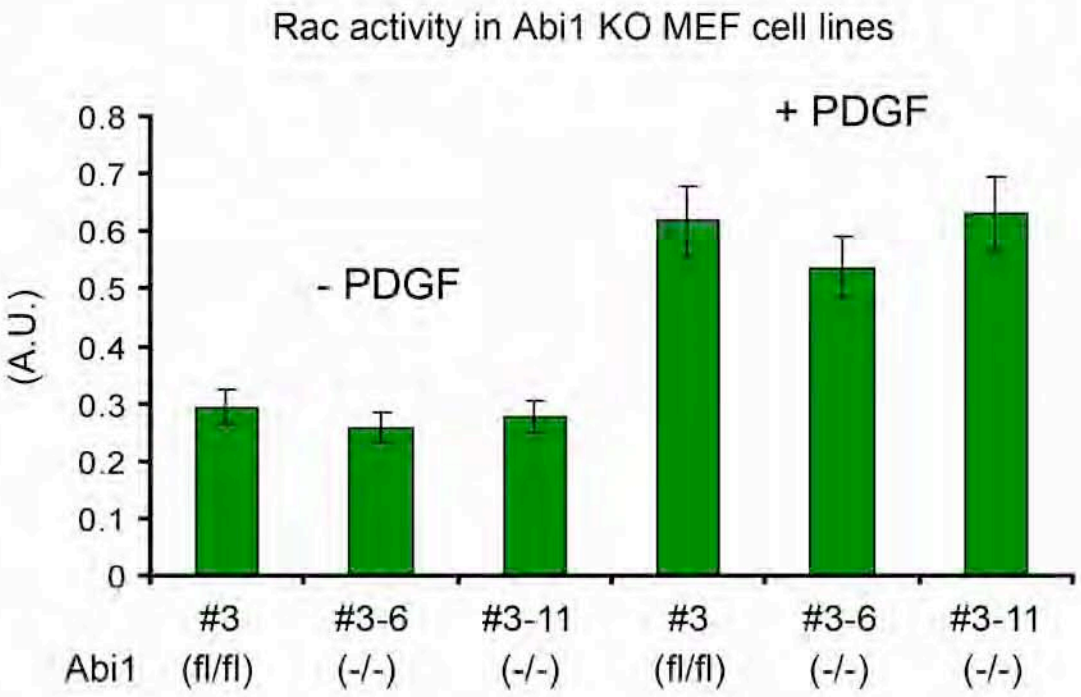
Rac activity in Abi1 KO MEF cell lines
+ PDGF
- PDGF
(A.U.)
0.8
0.7
0.6
0.5
0.4
0.3
0.2
0.1
0
#3
#3-6
#3-11
#3
#3-6
#3-11
Abi1
(fl/fl)
(-/-)
(-/-)
(fl/fl)
(-/-)
(-/-)

Figure 4

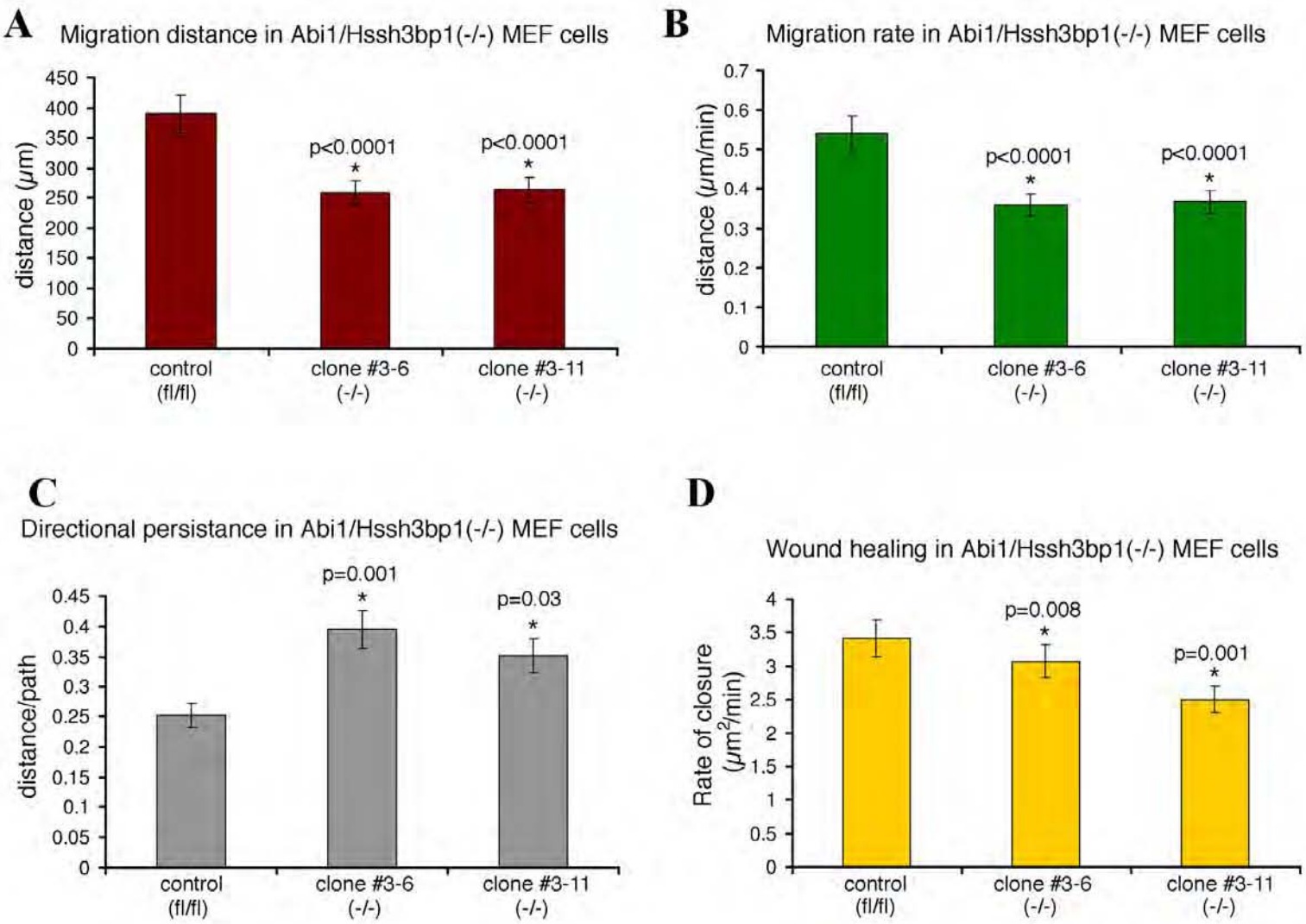
A
Migration distance in Abi1/Hssh3bp1(-/-) MEF cells
distance (μm)
450
400
350
300
250
200
150
100
50
0
p<0.0001
*
p<0.0001
*
control (fl/fl)
clone #3-6 (-/-)
clone #3-11 (-/-)
B
Migration rate in Abi1/Hssh3bp1(-/-) MEF cells
distance (μm/min)
0.7
0.6
0.5
0.4
0.3
0.2
0.1
0
p<0.0001
*
p<0.0001
*
control (fl/fl)
clone #3-6 (-/-)
clone #3-11 (-/-)
C
Directional persistance in Abi1/Hssh3bp1(-/-) MEF cells
distance/path
0.45
0.4
0.35
0.3
0.25
0.2
0.15
0.1
0.05
0
p=0.001
*
p=0.03
*
control (fl/fl)
clone #3-6 (-/-)
clone #3-11 (-/-)
D
Wound healing in Abi1/Hssh3bp1(-/-) MEF cells
Rate of closure (μm²/min)
4
3.5
3
2.5
2
1.5
1
0.5
0
p=0.008
*
p=0.001
*
control (fl/fl)
clone #3-6 (-/-)
clone #3-11 (-/-)
E
control (fl/fl)
clone #3-6
clone #3-11
0 min.
720 min.

Figure 5

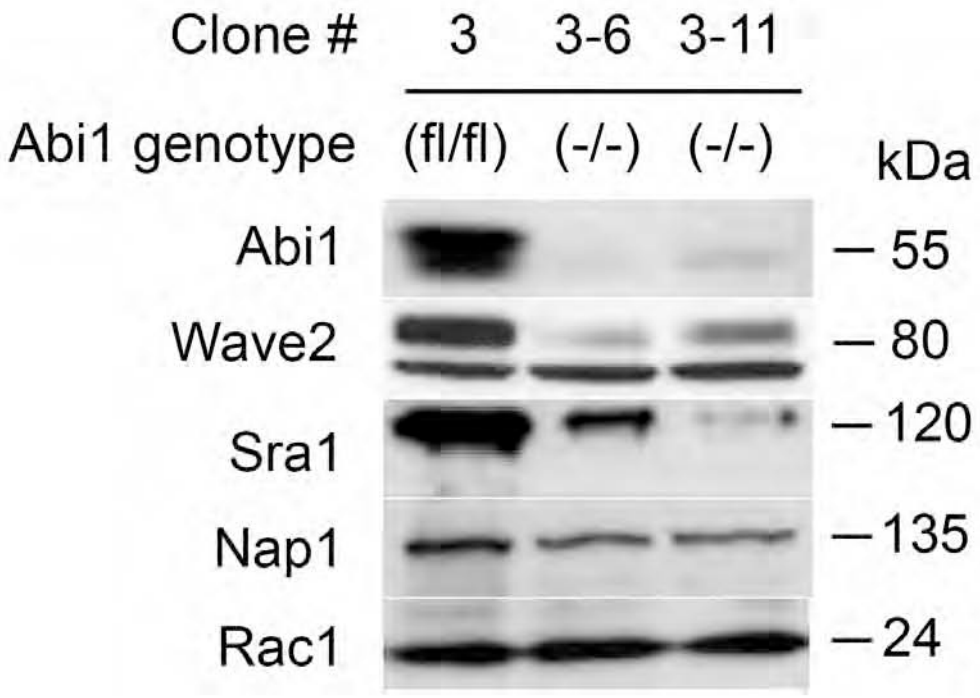
Clone #
3
3-6
3-11
Abi1 genotype
(fl/fl)
(-/-)
(-/-)
kDa
Abi1
Wave2
Sra1
Nap1
Rac1
55
80
120
135
24

Figure 6A

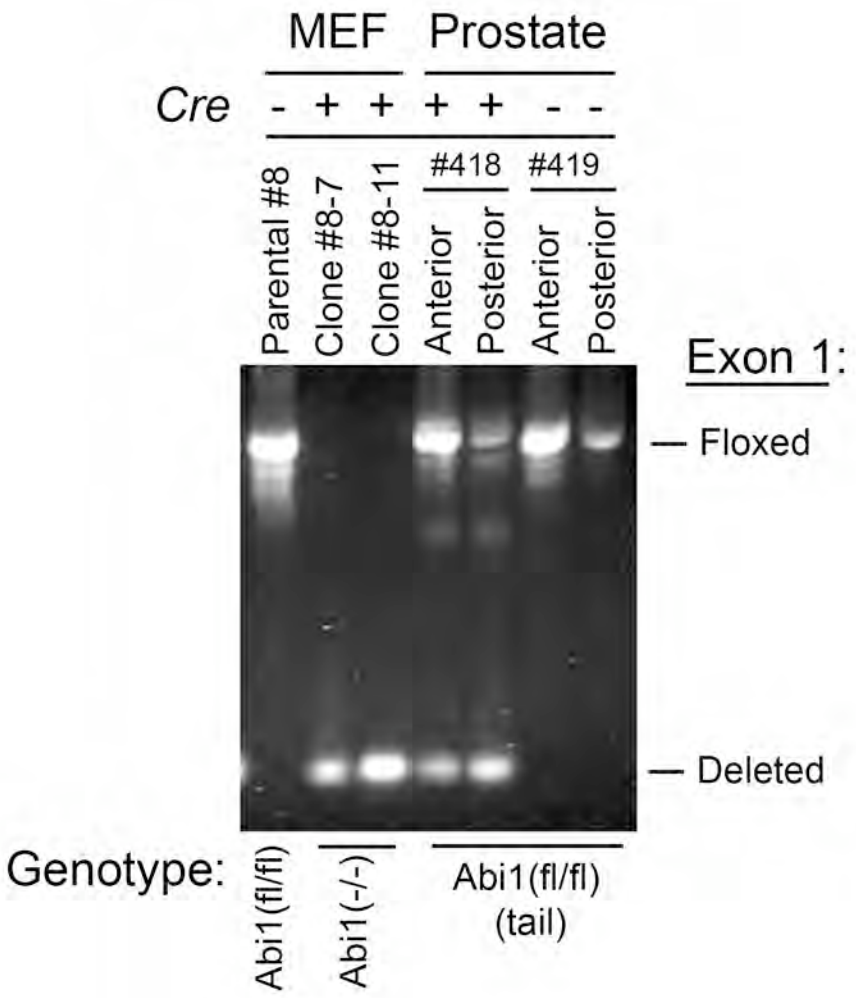
MEF
Prostate
Cre
- + + + + - -
#418
#419
Parental #8
Clone #8-7
Clone #8-11
Anterior
Posterior
Anterior
Posterior
Exon 1:
— Floxed
— Deleted
Genotype:
Abi1(fl/fl)
Abi1(-/-)
Abi1(fl/fl)
(tail)

Figure 6B

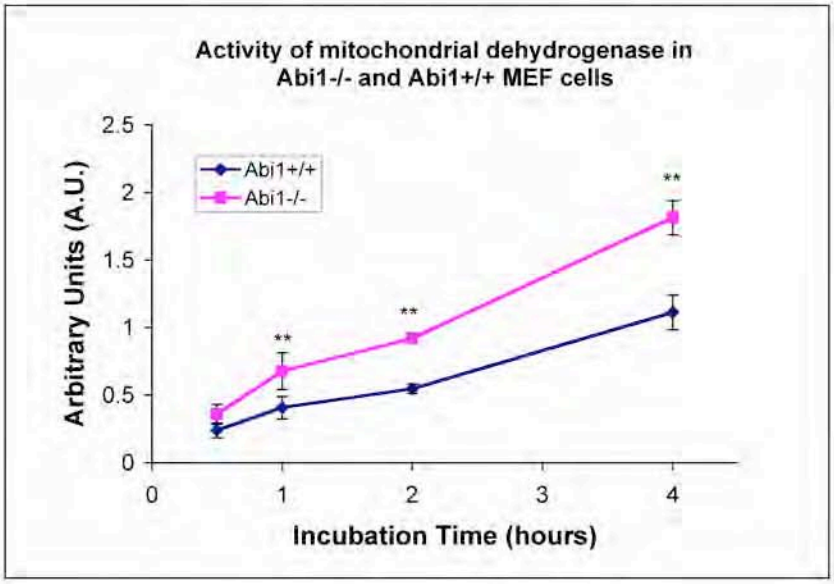
Activity of mitochondrial dehydrogenase in Abi1-/- and Abi1+/+ MEF cells
Arbitrary Units (A.U.)
Incubation Time (hours)
Abi1+/+
Abi1-/-
2.5
2
1.5
1
0.5
0
0
1
2
3
4
**
**
**

Abi1/Hssh3bp1 phosphotyrosine-SH2 domain screening document

SH2 profiling of Abi-1 peptides

Objective: To perform SH2 screen for tyrosine phosphorylation sites of c-Abl regulator Abi1 using biotinylated phosphopeptides.

1. Sample
   1 pY213 VKPPTVPNDpYMTSP (provided in solution)
   2 Y213 VKPPTVPNDYMTSP (provided in solution)
   3 pY213v2 PTVPNDpYMTSPARL (lyophilized)
   4 F213v2 PTVPNDFMTSPARL (lyophilized)
   5 pY421 PPPPPPPVDpYDYEE (lyophilized)
   6 Y421 PPPPPPPVDYDYEE (lyophilized)
2. SH2 screening (Expt. R1-3)
   Peptide solution were spotted on a nitrocellulose membrane for SH2 domain screening (method described in Mol Cell 26,6,899). The binding experiment was repeated and signal intensity was quantified using a densitometry (Fig. 1-4).
3. Affinity constant (Expt. R4)
   Based on the screening result, positive SH2 domains were selected and saturation-binding assay performed for affinity determination (Fig 5-6).
4. Result
   Solubilization of peptides: all lyophilized peptides were easily soluble in Tris pH6.8 buffer, although F213 and Y213 became clouded in the sample loading buffer.

   Immobilization: obviously pY213v2/F213 are superior than others in immobilization (Fig. 1 upper panel). To load the peptides as equivalent as possible, pY213/Y213/pY421/Y421 were concentrated by vacuum drier prior to spotting although the effort ended up with little improvement (Expt. R2-3).

   SH2 binding preferences: three consecutive SH2 screens were performed (Expt. R1-R3). Since optimization of assay condition had been attempted during the experiments, minor assay conditions are not necessarily identical, e.g., sample loading amount, probe concentration, etc, but averaged values clearly detected an unique SH2 binding preference of each peptide (Fig.4).

   Is Abl the best ligand for pY213?: the short answer is, at least from this experiment, No. Both screening result and affinity constant indicate that Abl is indeed a good ligand for pY212 among many other SH2 domains but there are multiple SH2 domains with higher affinity including Arg, CblB, and Vav2.

   Regarding SH2 binding motifs: pY213 favorably meets Cbl consensus, NXpYXXXP; Abl, PI3K, and Vav would prefer pYMX motif; whereas not meets Crk consensus. pY421 contains multiple acidic residues after pTyr that may attract Src family SH2s. Fes/Fer's affinity to this site was unexpected.

Expt. Kotula R1

Figure 1

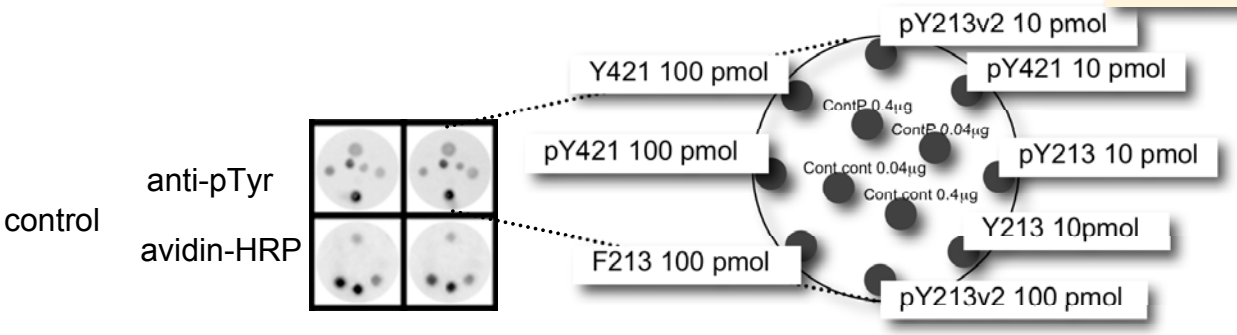

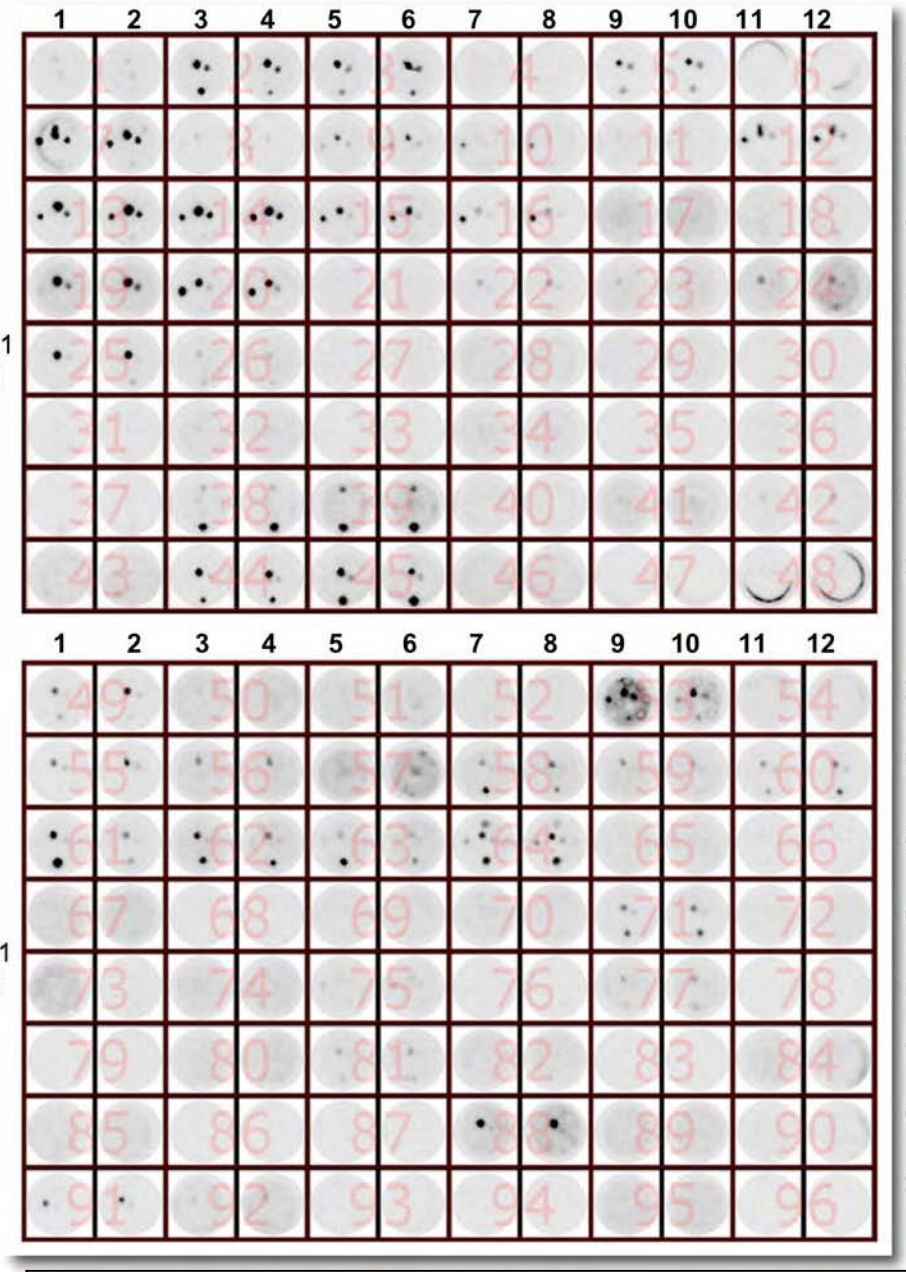

R1 Probe ID	
1 GST	49 Cten
2 hAbl	50 Rin2
3 mAbl	51 Rin3
4 mAbl_R174K	52 SOCS1
5 Arg	53 Nap4
6 Slap	54 CIS1
7 Lck	55 Nck
8 Src	56 Nck2
9 Src_chick	57 SHP-1(NC)
10 Lyn	58 mSHP-2(NC)
11 Blk	59 mSHP-2(N)
12 Fgr	60 p85a(NC)
13 Yes	61 p85b(NC)
14 FynA	62 p55g(NC)
15 FynT	63 Vav1
16 Hck	64 Vav2
17 SH2D5	65 Vav3
18 Ptk70	66 SH2-B
19 Brk	67 SH2B-RK
20 Frk	68 Lnk
21 Grap	69 Bks
22 Grb2	70 ShcA
23 Grap2	71 mSck/ShcB
24 Grb2+3	72 mShcC
25 Csk	73 ShcD
26 Matk	74 Fes
27 mSyk(NC)	75 Fer
28 mSyk(N)	76 Nsp2
29 Zap70(NC)	77 Gap(NC)
30 Zap70(C)	78 Plcg1(NC)
31 Grb14	79 Plcg2(NC)
32 Grb7	80 SHIP1
33 Grb10	81 SHIP2
34 HSH2	82 EAT2
35 Vrap	83 SAP
36 SH2A	84 mMist
37 CblA	85 mMist RK
38 CblB	86 SLP76
39 CblC	87 SLnk
40 Bks	88 Tec
41 Brdg1	89 Btk
42 SH3BP2	90 Txk
43 Supt6h	91 Bmx
44 Crk	92 Emt
45 CrkL	93 SHE
46 Tensin	94 SHF
47 Tem6	95 SHD
48 Tenc1	96 Shb

In expt R1, 10 pmol or 100 pmol of peptides was applied and immobilization status was evaluated by avidin-HRP and pTyr antibody. pY213/F213v2 well bound to the filter over the other peptides.

Expt. Kotula R2

Figure 2

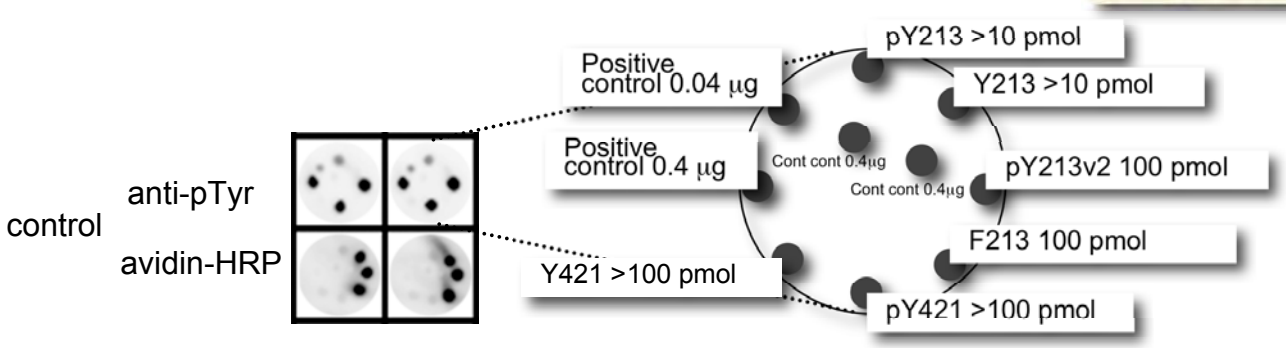

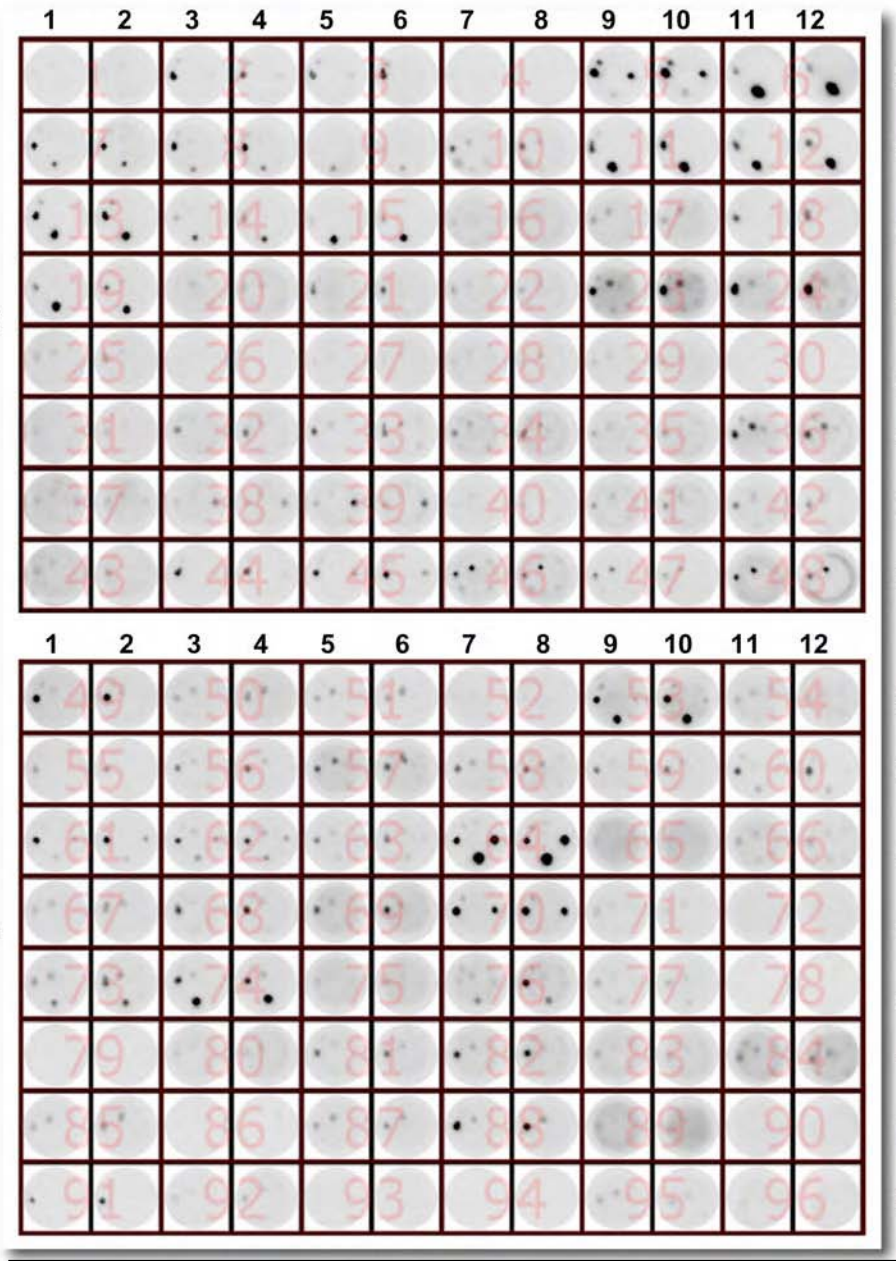

R2 Probe ID	
1 GST	49 Cten
2 hAbl	50 Rin2
3 mAbl	51 Rin3
4 mAbl_R174K	52 SOCS1
5 Arg	53 Nap4
6 Lck	54 CIS1
7 Src	55 Nck
8 Src_chick	56 Nck2
9 Lyn	57 SHP-1(NC)
10 Blk	58 mSHP-2(NC)
11 Fgr	59 mSHP-2(N)
12 Yes	60 p85a(NC)
13 FynA	61 p85b(NC)
14 FynT	62 p55g(NC)
15 Hck	63 Vav1
16 SH2D5	64 Vav2
17 Ptk70	65 Vav3
18 Brk	66 SH2-B
19 Frk	67 SH2B-RK
20 Grap	68 Lnk
21 Grb2	69 ShcA
22 Grap2	70 mSck/ShcB
23 Grb2+3	71 mShcC
24 Csk	72 ShcD
25 Matk	73 Fes
26 mSyk(NC)	74 Fer
27 mSyk(N)	75 Nsp2
28 mSyk(C)	76 Gap(NC)
29 Zap70(NC)	77 PLCG1 SH23
30 Zap70(C)	78 Plcg1(NC)
31 Grb14	79 Plcg2(NC)
32 Grb7	80 SHIP1
33 Grb10	81 SHIP2
34 HSH2	82 EAT2
35 Vrap	83 SAP
36 SH2A	84 mMist
37 CblA	85 mMist RK
38 CblB	86 SLP76
39 CblC	87 SLnk
40 Bks	88 Tec
41 Brdg1	89 Btk
42 SH3BP2	90 Txk
43 Supt6h	91 Bmx
44 Crk	92 Emt
45 CrkL	93 SHE
46 Tensin	94 SHF
47 Tem6	95 SHD
48 Tenc1	96 Shb

To increase sample loading of pY213 and pY421, peptide solutions were concentrated by a vacuum drier and then applied onto a membrane. Although avidin-HRP still dominantly detected pY213v2/F213, pTyr antibody detected equivalent level of phosphorylation for pY213v2 and pY412.

Expt. Kotula R3

Figure 3

SH2 domain screening was repeated with optimized assay condition.

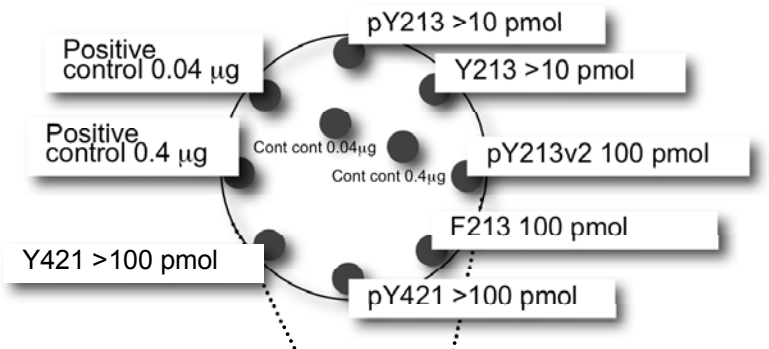

Expt R3 Plate 1

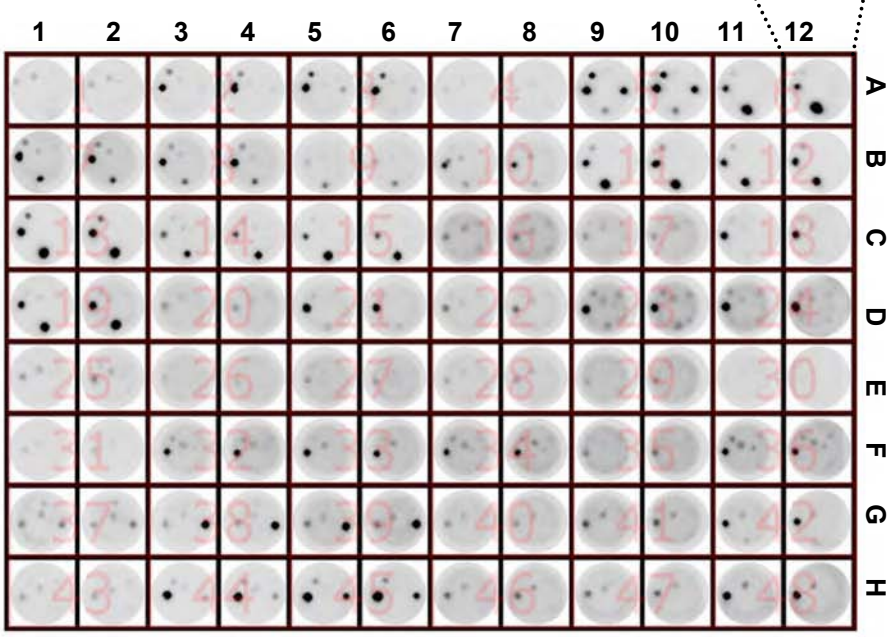

Expt R3 Plate 2

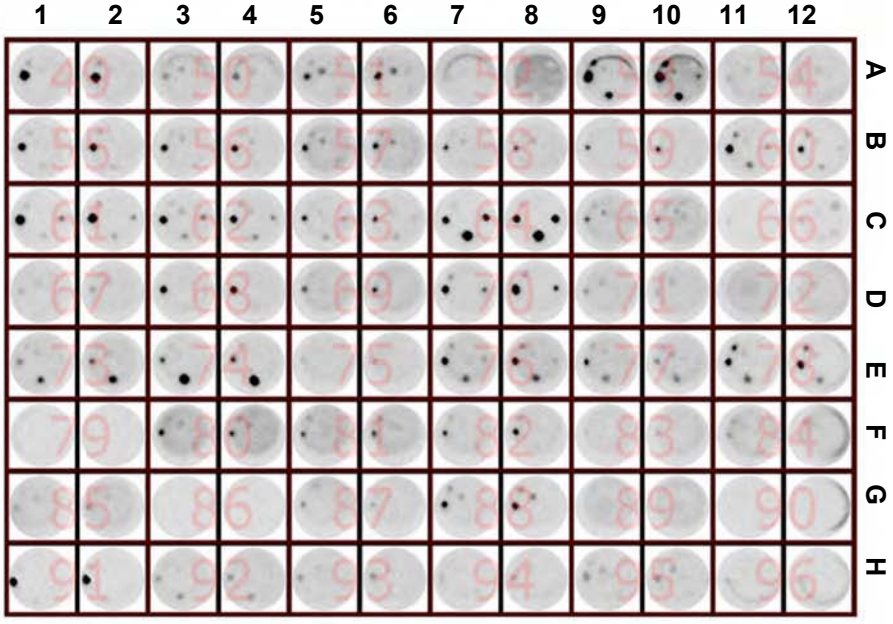

R3 Probe ID	
1 GST	49 Cten
2 hAbl	50 Rin2
3 mAbl	51 Rin3
4 mAbl_R174K	52 SOCS1
5 Arg	53 Nap4
6 Lck	54 CIS1
7 Src	55 Nck
8 Src_chick	56 Nck2
9 Lyn	57 SHP-1(NC)
10 Blk	58 mSHP-2(NC)
11 Fgr	59 mSHP-2(N)
12 Yes	60 p85a(NC)
13 FynA	61 p85b(NC)
14 FynT	62 p55g(NC)
15 Hck	63 Vav1
16 SH2D5	64 Vav2
17 Ptk70	65 Vav3
18 Brk	66 SH2-B
19 Frk	67 SH2B-RK
20 Grap	68 Lnk
21 Grb2	69 ShcA
22 Grap2	70 mSck/ShcB
23 Grb2+3	71 mShcC
24 Csk	72 ShcD
25 Matk	73 Fes
26 mSyk(NC)	74 Fer
27 mSyk(N)	75 Nsp2
28 mSyk(C)	76 Gap(NC)
29 Zap70(NC)	77 PLCG1 SH23
30 Zap70(C)	78 Plcg1(NC)
31 Grb14	79 Plcg2(NC)
32 Grb7	80 SHIP1
33 Grb10	81 SHIP2
34 HSH2	82 EAT2
35 Vrap	83 SAP
36 SH2A	84 mMist
37 CblA	85 mMist RK
38 CblB	86 SLP76
39 CblC	87 SLnk
40 Bks	88 Tec
41 Brdg1	89 Btk
42 SH3BP2	90 Txk
43 Supt6h	91 Bmx
44 Crk	92 Emt
45 CrkL	93 SHE
46 Tensin	94 SHF
47 Tem6	95 SHD
48 Tenc1	96 Shb

Expt. Kotula R1-3
Quant

Figure 4

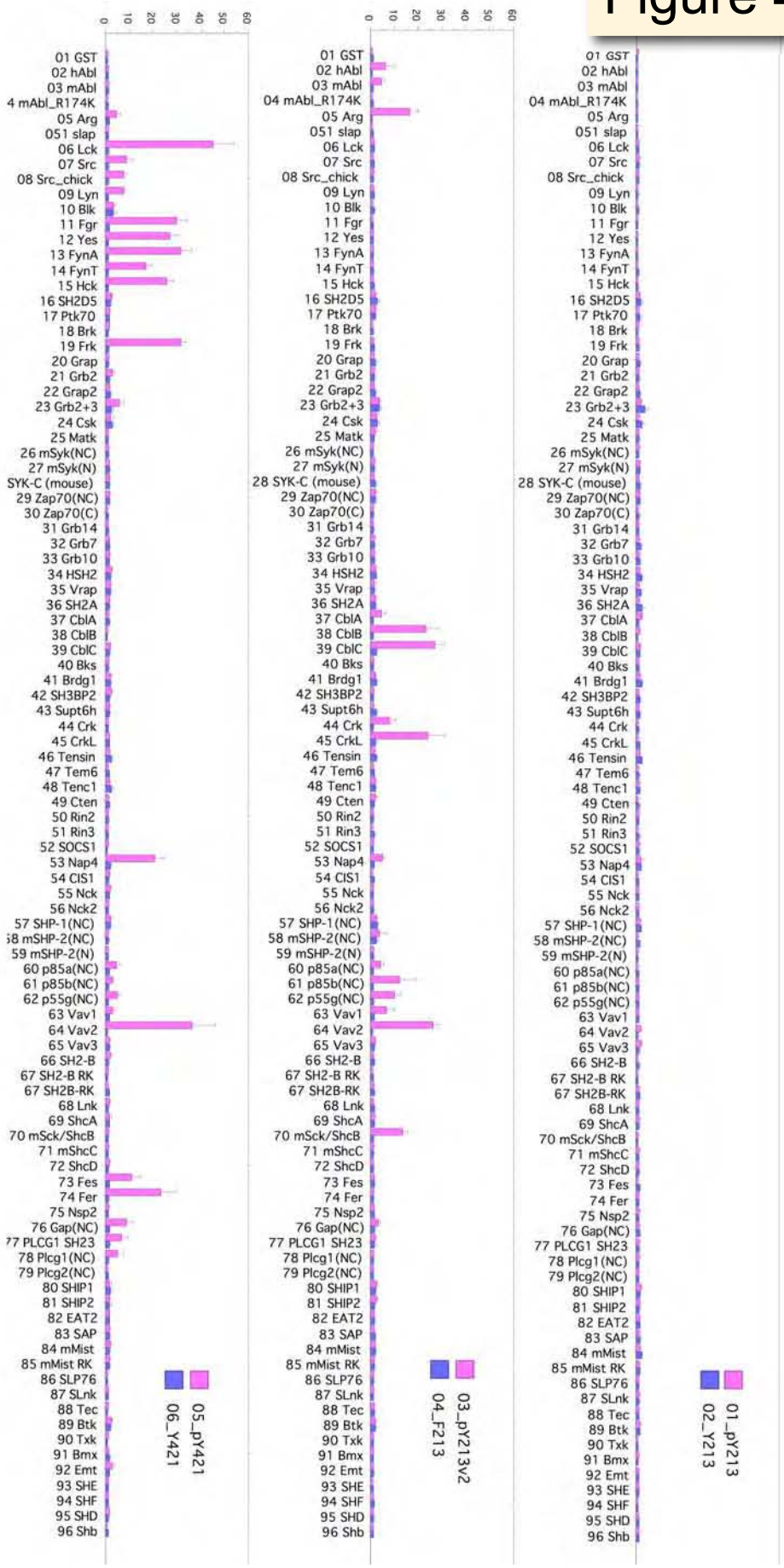

Average signal intensity based on three independent SH2 screen experiments is shown. Due to their poor immobilization efficiency, specific SH2 binding was not detected with pY213/Y213 peptides, while pY213v2 and pY421/Y421 peptides displayed distinct SH2 binding preferences. SH2 domains of Abl/Arg, CBLs, CRKs, PI3Ks,VAVs, and Sck proteins were selected by pY213v2 peptide; Src family proteins, Frk, Nap4, Vav2, Fer/Fes, Gap, and PLCγ1 were selected by pY421.

Expt. Kotula R4

Figure 5

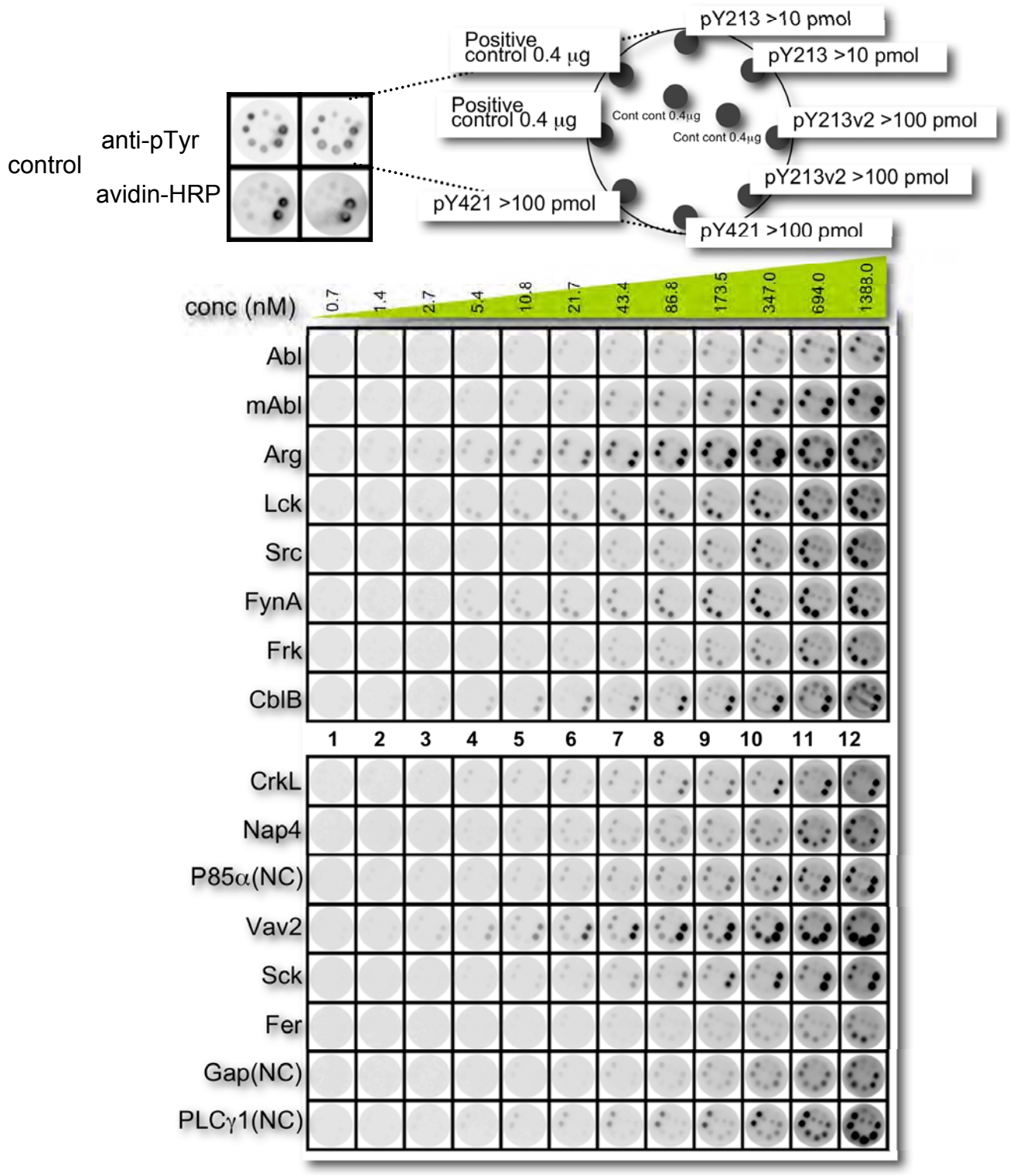

Based on the SH2 screen, representative 16 SH2 domains were selected and binding affinity was evaluated by a saturation-binding experiment. Concentration used are shown on top.

Expt. Kotula R4
Constant

Figure 6

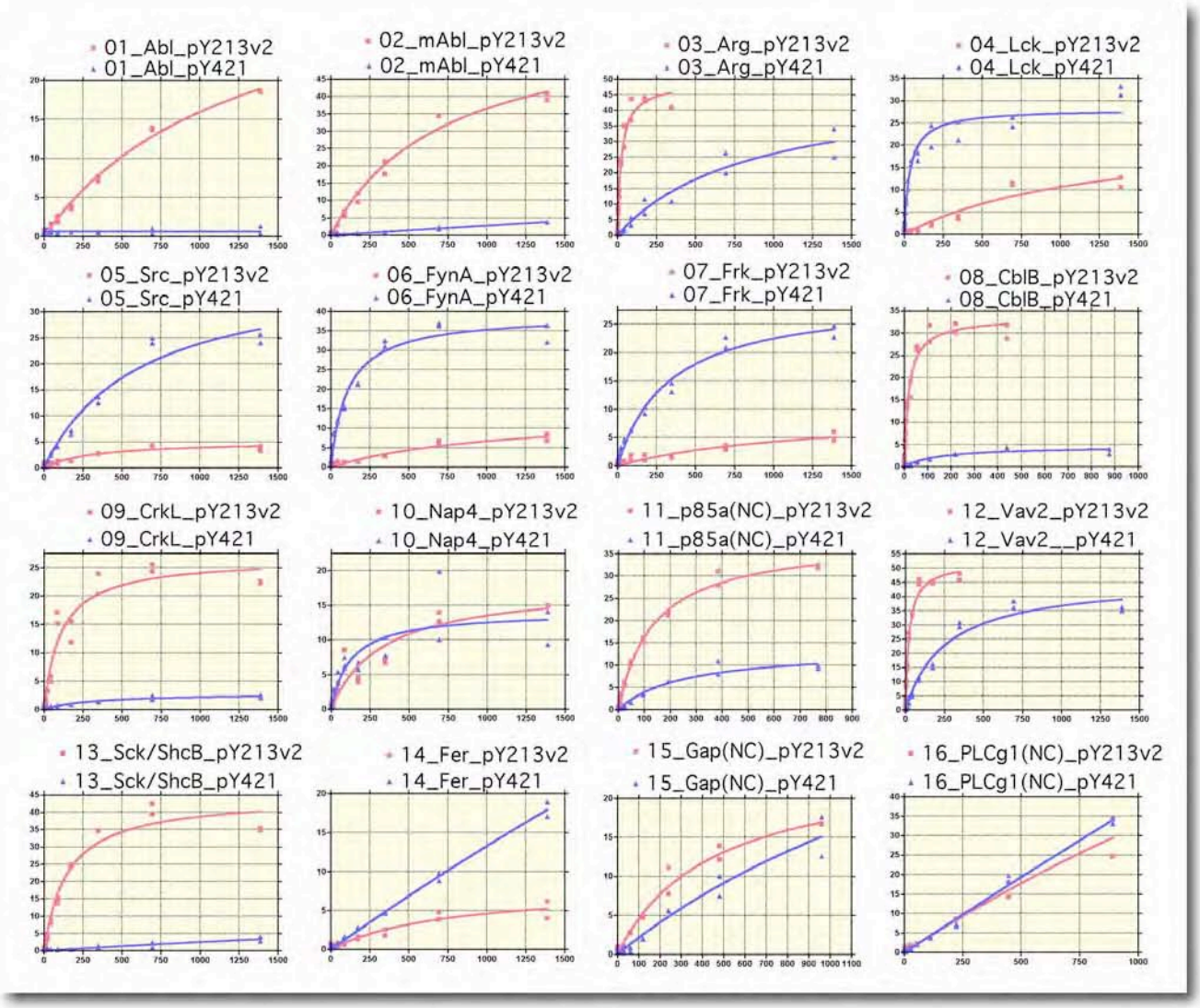

	Kd (nM)	
SH2	**pY213v2**	**pY421**
Abl	**1259**	**UD**
mAbl	**725.3**	**UD**
Arg	**25.08**	**844.5**
Lck	**1207**	**36.42**
Src	**UD**	**612.5**
FynA	**UD**	**108.2**
Frk	**UD**	**329.7**
CblB	**19.52**	**UD**
CrkL	**106.8**	**UD**
Nap4	**UD**	**UD**
p85α(NC)	**134.8**	**240.6**
Vav2	**23.19**	**255**
Sck/ShcB	**148.7**	**UD**
Fer	**UD**	**UD**
Gap(NC)	**441.5**	**UD**
PLCγ1(NC)	**UD**	**UD**

UD, undefined

Dissociation constant (Kd) was estimated by the non-linear curve fitting with PRISM 4.0 (GraphPad).